INFORMATION TO USERS

This manuscript has been reproduced from the microfilm master. UMI films the text directly from the original or copy submitted. Thus, some thesis and dissertation copies are in typewriter face, while others may be from any type of computer printer.

The quality of this reproduction is dependent upon the quality of the copy submitted. Broken or indistinct print, colored or poor quality illustrations and photographs, print bleedthrough, substandard margins, and improper alignment can adversely affect reproduction.

In the unlikely event that the author did not send UMI a complete manuscript and there are missing pages, these will be noted. Also, if unauthorized copyright material had to be removed, a note will indicate the deletion.

Oversize materials (e.g., maps, drawings, charts) are reproduced by sectioning the original, beginning at the upper left-hand corner and continuing from left to right in equal sections with small overlaps.

ProQuest Information and Learning
300 North Zeeb Road, Ann Arbor, Mi 48106-1346 USA
800-521-0600

Computational Studies on the Effects of Heteroatom Substitution in Delocalized Pi Systems

Eric Carroll Brown

A dissertation submitted in partial fulfillment of the requirements for the degree of

Doctor of Philosophy

University of Washington

2002

Program Authorized to Offer Degree: Chemistry

UMI Number: 3072064

UMI Microform 3072064

ProQuest Information and Learning Company
300 North Zeeb Road
P.O. Box 1346
Ann Arbor, MI 48106-1346

In presenting this dissertation in partial fulfillment of the requirements for the Doctoral degree at the University of Washington, I agree that the Library shall make its copies freely available for inspection. I further agree that extensive copying of the dissertation is allowable only for scholarly purposes, consistent with "fair use" as prescribed in the U. S. Copyright Law. Requests for copying or reproduction of this dissertation may be referred to Proquest Information and Learning, 300 North Zeeb Road, Ann Arbor, MI 48106-13-46, to whom the author has granted "the right to reproduce and sell (a) copies of the manuscript in microform and or (b) printed copies of the manuscript made from microform."

Signature Eric C Brown

Date December 2, 2002

This is to certify that I have examined this copy of a doctoral dissertation by

Eric Carroll Brown

and have found that it is complete and satisfactory in all respects,
and that any and all revisions required by the final
examining committee have been made.

Chair of Supervisory Committee:

Weston T. Borden

Reading Committee:

Weston T. Borden

Bart E. Kahr

Bruce H. Robinson

Date: December 2, 2002

University of Washington

Abstract

Computational Studies on the Effects of Heteroatom Substitution
in Delocalized Pi Systems

Eric Carroll Brown

Chair of the Supervisory Committee:
Professor Weston T. Borden
Chemistry

The effects of heteroatom (or group) substitution in several delocalized π systems are discussed. A brief review of the various types of heteroatom substitutions which preserve an isoelectronic valence space is presented. In the second chapter, a rationalization is presented for why silabenezene readily dimerizes, whereas the isovalent phosphabenzene does not. The next chapter is concerned with heteroatom substitution of the central carbon atom of trimethylenemethane radical cation and trimethylenemethane radical anion, both of which possess doublet ground states. The question addressed is whether an isovalent species with heteroatom substitution might have a quartet ground state. In the final chapter, it is predicted that the bishomoaromatic stabilization of several heteroatom-substituted semibullvalenes is quite small, despite the fact that these molecules have high-symmetry equilibrium geometries.

TABLE OF CONTENTS

LIST OF FIGURES

Figure Number

Page

LIST OF TABLES

LIST OF SYMBOLS

—	sigma (σ) bond, i.e. a single bond
=	sigma (σ) plus pi (π) bond, i.e. a double bond
≡	sigma (σ) plus two pi ($\pi_1 + \pi_2$) bonds, i.e. a triple bond
ΔH	change in enthalpy (in the standard state, unless otherwise noted)
DH	homolytic bond dissociation enthalpy (BDE)
E	energy of a state
Ψ	state wave function
ψ	molecular orbital
φ	atomic orbital

Acknowledgments

I wish to express my sincere appreciation to the American people who have funded this research through grants administered by the National Science Foundation. The research in each chapter was performed in collaboration with my advisor, Professor Weston T. Borden. Mr. Daven K. Henze also collaborated on the research reported in Chapter IV.

I. Introduction: Heteroatoms in Organic Molecules

It is made clear in most textbooks that the discipline of organic chemistry is based on carbon and the molecules it forms. Thus, it is not surprising that many organic chemists view other elements (*heteroatoms*), especially those of the first and second periods, as carbon atoms whose electronegativities and electron counts have been perturbed.

For example, in forming bonds carbon and silicon both contribute four valence electrons. Thus, one might expect the geometries about carbon and silicon to be similar, e.g. tetrahedral centers in CH_3CH_3 and CH_3SiH_3 and planar centers in $CH_2{=}CH_2$ and $CH_2{=}SiH_2$. However, since silicon is less electronegative than carbon, it is expected that the energetically-optimal electron distribution would reflect this difference. Indeed, the magnitude of the dipole moment of CH_3SiH_3 is found to lie in the direction of the carbon atom ($H_3C{\leftarrow}SiH_3$).[1,2]

It is also possible to substitute a heteroatom for a C-H group in such a way that the total number of valence electrons does not change. Substitution of a CH group in methane and in benzene (C_6H_6) with a nitrogen atom affords, respectively, ammonia and pyridine (C_5H_5N).[3]

Substitution of a carbon atom by an isoelectronic atomic ion (or group) represents another way to generate a molecule with a geometry that is similar to the parent. For example, CH_4 is a tetrahedral molecule, as are NH_4^+ and BH_4^-.

In the above comparisons, while each pair are structurally similar, shape is about all they have in common. Indeed, their reactivities and their other chemical properties may be radically different. For example, CH_2=SiH_2 readily dimerizes, but CH_2=CH_2 does not. Benzene and pyridine are both highly aromatic and inert to electrophilic aromatic substitution, but the latter possesses a dipole moment and is a base with a particularly foul odor. Like CH_4, NH_4^+ and BH_4^- have no dipole moment; but, since they are charged species, they readily associate with counterions, e.g. $NH_4^+Cl^-$ and $Na^+BH_4^-$.

This dissertation describes several examples of how substituting various delocalized hydrocarbons with heteroatoms affects their properties, including their reactivity and stability and ground state electronic configurations. Chapter II provides an explanation as to why silabenzene (C_5H_5SiH) readily dimerizes; whereas benzene, pyridine, and phosphabenzene (C_5H_5P) do not. Chapter III presents a discussion of why *planar* heteroatom derivatives, that are isoelectronic with trimethylenemethane (TMM, C_4H_6) radical cations, do not have a quartet ground state, whereas certain planar heteroatom derivatives which are isolectronic with the radical anion of TMM may have quartet ground states.

The discovery of neutral homoaromatics (*vide infra*) remains an active area of experimental and theoretical focus. Chapter IV is concerned with the quantification of the bishomoaromatic stabilization in various semibullvalenes that have been substituted with heteroatoms, especially at the 1 and 5 positions.

The results presented in this dissertation were obtained from electronic structure calculations based on both wave functions[4] and Density Functional Theory.[5] Computational methods, known to give reasonable relative energies and properties for each type of molecule that is discussed in this dissertation, were employed.

II. What Accounts for the Difference Between Silabenzene and Phosphabenzene in Stability Toward Dimerization?

Introduction

A striking example of the difference in reactivities between compounds containing Si=C[8] and P=C[7] bonds[8] is provided by the comparison between silabenzene and phosphabenzene. For example, silabenzenes dimerize at very low temperatures,[9] although bulky substituents can be used to inhibit[10] or prevent[11] these bimolecular reactions. In stark contrast, phosphabenzene[12] is highly resistant to dimerization; and it only undergoes a Diels-Alder reaction with hexafluoro-2-butyne after two days of heating at 100° C.[13]

The development of density functional theory (DFT) has made it practical to perform accurate calculations on the dimerization of phosphabenzene and silabenzene and, hence, to explore the causes of the striking difference in reactivity between these two molecules. In this chapter, I report the results of B3LYP/6-31G* calculations which find that this difference in reactivity has a thermodynamic origin. These calculations also show the major cause of the very large difference in calculated heats of dimerization is not the difference between the strengths of the Si-C and P-C π bonds in the reactants that are broken but, instead, the difference between the strengths of the σ bonds to silicon and to phosphorus that are formed in the products.

Computational Methodology

All calculations were carried out with the *Gaussian 98* suite of programs[14] using the 6-31G* basis set.[15] Geometry optimizations were performed utilizing Becke's hybrid three-parameter exchange functional and the nonlocal correlation functional of Lee, Yang, and Parr (B3LYP).[16] A vibrational analysis was performed at each stationary point found, in order to confirm its identity as an energy minimum or a transition structure. The harmonic frequencies were used, without scaling, to calculate the zero-point energy and thermal corrections necessary to obtain the enthalpies of reaction.

Results and Discussion

I began by calculating the enthalpy of Diels-Alder dimerization of two moles of each heterobenzene. This reaction is shown in eq 1 for silabenzene (**SB**) and in eq 2 for phosphabenzene (**PB**).

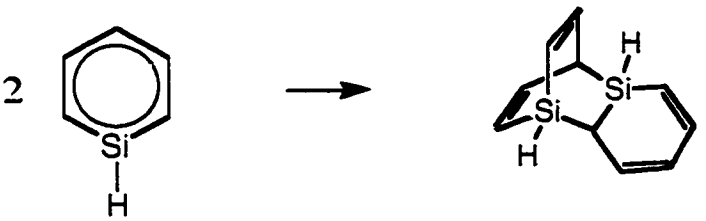

eq 1

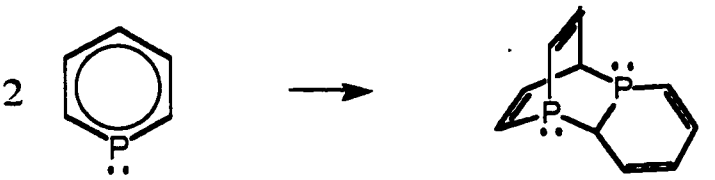

eq 2

As expected, the dimerization of **SB** was computed to be exothermic, with ΔH = -21.5 kcal mol. In contrast, the dimerization of **PB** was calculated to be highly endothermic, with ΔH = 32.6 kcal mol, consistent with the failure to observe **PB** dimerization.

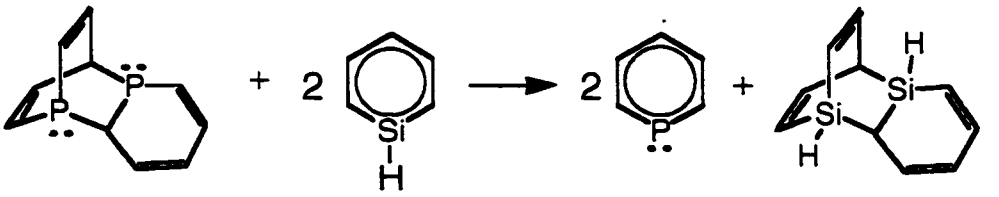

eq 3

The isodesmic reaction in eq 3 represents the difference between the heats of dimerization of **SB** and **PB** and is, therefore, extremely exothermic; ΔH = -54.1 kcal mol. An obvious question is whether the considerable exothermicity of the reaction in eq 3 is due primarily to a difference between the strengths of the Si-C and P-C π bonds in the reactants, which are broken in the dimerization reactions, or to a difference between the

strengths of the Si-C and P-C σ bonds that are formed in the Diels-Alder dimerization products.

In order to answer this question most conveniently, I chose to model the formation of the Si-C and P-C bonds in eq 1 and eq 2 with the Si-H, P-H, and C-H bonds formed when hydrogen is added to a bond between carbon and the heteroatom in **SB** and **PB**. For this model to be valid, the difference between the heats of hydrogen addition to two moles each of **SB** and **PB**, which is given by twice the enthalpy of the isodesmic reaction in eq 4, should be comparable to the difference between the heats of dimerization, which is given by eq 3.

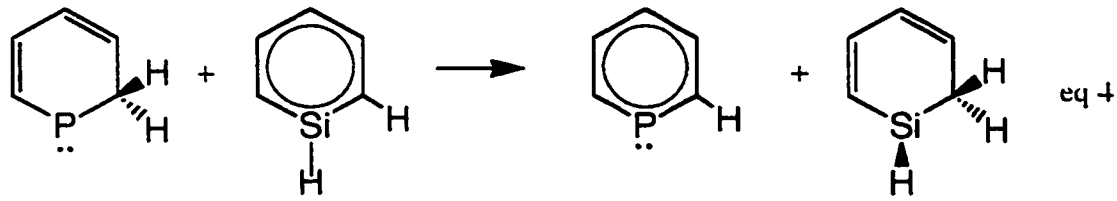

eq 4

The enthalpy of the reaction in eq 4 is calculated to be ΔH = - 24.0 kcal mol.[17] Twice this value differs by only 11% from the value of ΔH = -54.1 kcal mol for the reaction in eq 3. Therefore, determining the origins of the difference between the heats of hydrogen addition to **SB** and **PB** provides not only a tractable but also a reasonable way to try to understand the reasons for the very large difference between the heats of dimerization.

Relative π Bond Strengths

Perhaps the most obvious of the possible sources of the 24.0 kcal/mol difference between the heats of hydrogen addition to an Si=C bond in **SB** and to a P=C bond in **PB** is that the former type of π bond is much weaker than the latter. Employing Benson's definition of π bond strengths,[18] I computed the Si-C and P-C π bond dissociation enthalpies in **SB** and **PB** as the enthalpies of the isodesmic reactions in, respectively, eq 5 and eq 6. The calculated value of DH^{298} π(Si-C) = 34.8 kcal/mol is only 2.6 kcal/mol smaller than that of DH^{298} π(P-C) = 37.4 kcal mol. This difference in π bond dissociation enthalpies contributes only about 10% of the difference between the heats of hydrogen addition to an Si=C bond in **SB** and a P=C bond in **PB**.

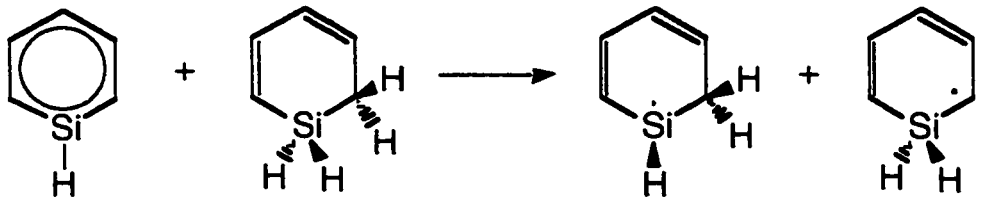

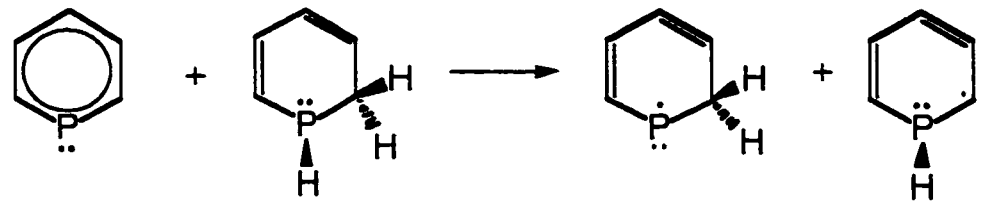

Another possible contributor to the calculated difference between the heats of hydrogen addition to **SB** and **PB** is the difference between the strengths of the C-H bonds

formed. This difference is given by the enthalpy of the isodesmic reaction in eq 7, which is calculated to be ΔH = 1.9 kcal/mol.

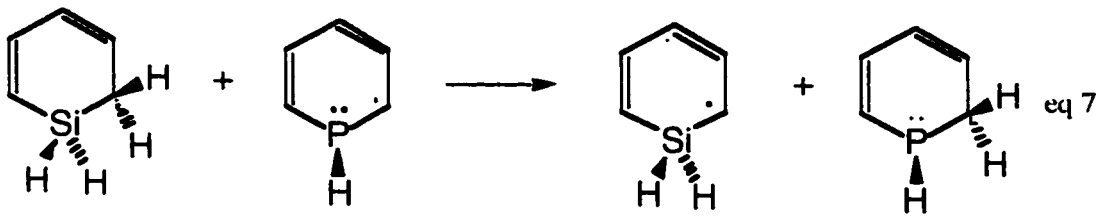

eq 7

The C-H bond formed upon addition of hydrogen to **SB** is slightly stronger than the C-H bond formed upon addition of hydrogen to **PB**, because the cyclohexadienyl radical is stabilized slightly more by the lone pair on the phosphorus atom than by hyperconjugation with the Si-H bonds. Brauman and coworkers have compared the experimental C-H bond dissociation enthalpies (BDEs) of $(CH_3)_4Si$ and $(CH_3)_3P$ and found that a C-H bond is stronger by *ca.* 3 kcal/mol in tetramethylsilane than in trimethylphosphine.[19] G2 calculations by Wiberg and Nakaji have found a similar difference between the C-H BDEs of CH_3SiH_3 and CH_3PH_2.[6c]

The greater stabilization of the cyclohexadienyl radical by phosphorus than by silicon also weakens the P-C π bond in **PB**, relative to the Si-C π bond in **SB**. The difference between cyclohexadienyl radical stabilization energies cancels if the difference between the strengths of the C-H bonds formed upon addition of hydrogen to **SB** and **PB** (which is given by the isodesmic reaction in eq 7) is subtracted from the difference between the π bond strengths (which is given by the difference between the enthalpies of

the reactions in eq 5 and eq 6). Subtracting eq 6 and eq 7 from eq 5 produces the isodesmic reaction in eq 8.

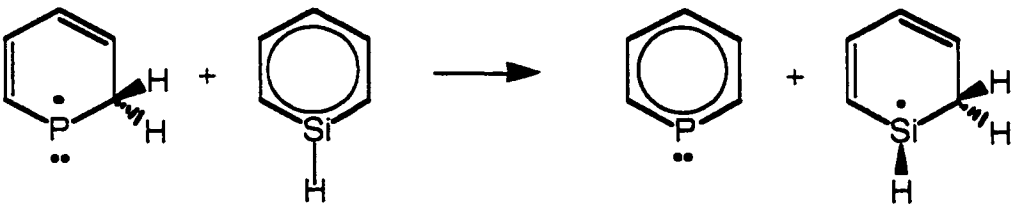

eq 8

This isodesmic reaction gives the difference between the enthalpies of adding a hydrogen atom to an *ortho* carbon of **SB** and of **PB**. This enthalpy difference is equal to ΔH = - 2.6 - 1.9 = - 4.5 kcal mol. If one assumes that, without selective stabilization of the cyclohexadienyl radical by the phosphorus lone pair, the strengths of the C-H bonds formed in the addition of hydrogen to **SB** and **PB** would be exactly the same, then 4.5 kcal mol represents the difference between the intrinsic strengths of the Si-C and P-C π bonds in **SB** and **PB**, when the weakening of the latter from radical stabilization by the phosphorus lone pair is ignored.

What accounts for the exothermicity of the isodesmic reaction in eq 8? It has been previously shown that pyramidalization of radical centers weakens the π bonds formed to them.[8c,20] Silyl radical centers prefer pyramidal geometries;[21] and, as in 1-silaallyl radical,[20d] maximizing conjugation with the adjacent double bond does not supply a driving force sufficient to induce the silyl radical in eq 8 to adopt a planar

geometry. Consequently, pyramidalization of this silyl radical weakens the Si-C π bond in **SB**, in which the silicon has a planar geometry.

The amount of energy by which the π bond in **SB** is weakened by the preference of the silyl radical in eq 8 for a pyramidalized geometry can easily be obtained by computing the amount of energy required to constrain the silicon in the radical to planarity. Decreasing the angle between the Si-H bond and the C-Si-C plane from its equilibrium value of 48.7° to 0° is calculated to increase the enthalpy of the radical in eq 8 by 4.2 kcal mol. Thus, the isodesmic reaction in eq 9, in which the silyl radical center is constrained to be planar, is almost thermoneutral. Therefore, if the reaction in eq 8 is taken to provide the best measure of the difference between the intrinsic strengths of the Si-C and P-C π bonds in, respectively, **SB** and **PB**, then the enthalpy of ΔH = - 0.3 kcal mol that is computed for the isodemic reaction in eq 9 shows these two types of π bonds apparently have almost exactly the same strengths when the silyl radical is constrained to planarity.

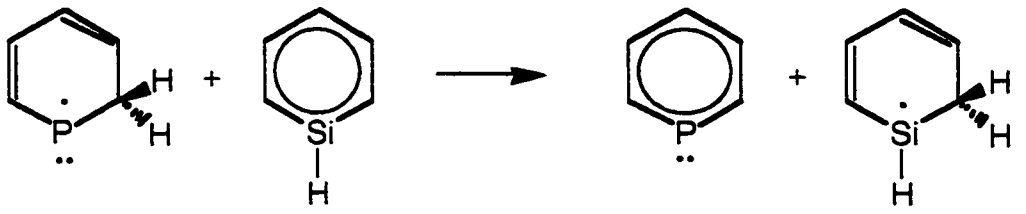

eq 9

The Difference Between Si-H and P-H σ Bond Strengths.

The reaction in eq 8 gives the difference between **SB** and **PB** in the strengths of the π bonds broken plus the C-H sigma bonds made upon addition of a hydrogen atom to an α carbon of each heterobenzene. The sum of these two differences amounts to only 4.5 kcal mol. The remainder of the 24.0 kcal mol difference between the heats of H_2 addition to **SB** and **PB** must be due, therefore, to a 19.5 kcal mol difference between the strengths of the Si-H and P-H bonds formed. Subtracting eq 8 from eq 4 gives eq 10; and the enthalpy of ΔH = -19.5 kcal mol for the isodesmic reaction in eq 10 is, indeed, equal to the difference between the BDEs of these two bonds.

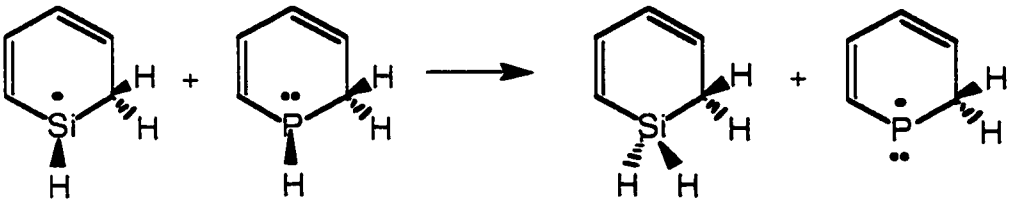

eq 10

In order to identify the origin(s) of the 19.5 kcal mol greater bond strength of the Si-H compared with the P-H bond, it is useful to consider a variant of the reaction in eq 10. The isodesmic reaction in eq 11, in which the silyl radical is constrained to planarity, is easier to analyze than the reaction in eq 10, because in eq 10 the phosphoryl radical, which is divalent and, hence, necessarily planar, is more delocalized than the pyramidal silyl radical. This difference between the two radicals in eq 10 is easily seen by inspection of the bond lengths in them, which are given in Figure 1.

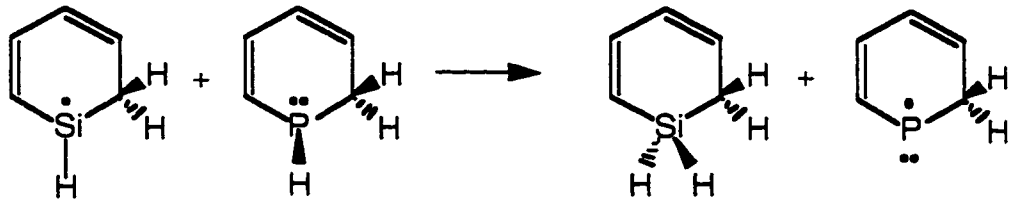

eq 11

Figure 1 also shows that the bond lengths in the planar silyl radical are close to those in the phosphoryl radical. The similar bond lengths in the two radicals in eq 11 suggests that the amounts of electron delocalization in them are similar too.

As already noted, constraining the silyl radical in the left hand side of eq 10 to planarity is computed to require 4.2 kcal/mol. Consequently, the exothermicity of the isodesmic reaction in eq 11 is ΔH = - 19.5 - 4.2 = -23.7 kcal/mol. This is the difference between the Si-H and P-H BDEs in the hydrogen addition products of **SB** and **PB**, when the silyl radical that forms the Si-H bond is constrained to be planar. This difference between the Si-H and P-H bond strengths accounts for all but 0.3 kcal/mol of the difference between the enthalpies of hydrogen addition to **SB** and **PB**.

Contributors to the Difference Between the Si-H and P-H Bond Strengths.

Why is the Si-H bond so much stronger than the P-H bond? The very large difference between silicon and phosphorus in the strengths of the bonds formed to hydrogen is particularly perplexing when it is recalled that in the first row of the periodic table N-H bonds are, in general, stronger than C-H bonds.[22]

It has been previously pointed out[8a] that an important contributor to the difference between the σ bond strengths in silanes and phosphines[8] is the difference between the hybridization of the bonds to silicon in the former and the bonds to phosphorus in the latter. The much greater amount of 3s character in the bonds formed by tetravalent silicon than by trivalent phosphorus[23] makes the former type of σ bonds stronger than the latter. For example, as shown in Table 1, B3LYP/6-31G* computes the difference between DH^{298} (H_3Si-H) = 90.0 kcal/mol and DH^{298} (H_2P-H) = 79.9 kcal/mol to be 10.1 kcal/mol.

As also shown in Table 1, an experimental value in the range, DH^{298} (H_3Si-H) = 91.7 ± 0.5 kcal/mol has been deduced for H_3Si-H.[24] The two experimental values of DH^{298} (H_2P-H) = 83.9[24] and 80.9[25] kcal/mol that have most recently been recommended for H_2P-H span a much wider range. The average of these two values, DH^{298} (H_2P-H) = 82.4 kcal/mol, differs from the value of DH^{298} (H_3Si-H) = 91.7 kcal/mol by 9.3 kcal/mol. This difference is slightly smaller than the B3LYP/6-31G* difference of DH^{298} (H_3Si-H) - DH^{298} (H_2P-H) = 10.1 kcal/mol.

Another way of evaluating the accuracy of the B3LYP/6-31G* energy difference between the H_3Si-H and H_2P-H BDEs is to compare this value with that computed by a very high quality *ab initio* method. For example, as shown in Table 1, G2 calculations[26] give DH^{298} (H_3Si-H) = 92.7 kcal/mol, and DH^{298} (H_2P-H) = 82.9 kcal/mol. The value of

9.8 kcal/mol for the difference between the H_3Si-H and H_2P-H BDEs, computed at this level of *ab initio* theory, is very close to the B3LYP/6-31G* value of 10.1 kcal/mol.

The difference in hybridization between silicon in SiH_4 and phosphorus in PH_3 contributes 10.1 kcal/mol to a B3LYP/6-31G* exothermicity of ΔH = - 23.7 kcal/mol for the isodesmic reaction in eq 11. Therefore, more than half of the difference between the Si-H and P-H BDEs, given by the enthalpy of this reaction, remains unaccounted for. What contributes the additional 13.6 kcal/mol to the exothermicity of the reaction in eq 11?

There are several possible contributors. The first is that the radical centers in eq 11 are both secondary. Therefore, rather than comparing the B3LYP/6-31G* BDEs of H_3Si-H and H_2P-H, a better comparison for the reaction in eq 11 would be the difference between the B3LYP/6-31G* BDEs of $(CH_3)_2SiH$-H and $(CH_3)_2P$-H. As shown in Table 1, the B3LYP/6-31G* difference between the BDEs of $(CH_3)_2SiH$-H and $(CH_3)_2P$-H is computed to be 14.6 kcal/mol. This difference is 4.5 kcal/mol larger than the B3LYP/6-31G* difference between the BDEs of H_3Si-H and H_2P-H.

The isodesmic reaction in eq 12 gives the difference between the Si-H BDE in silacyclohexane and the P-H BDE in phosphacyclohexane. The B3LYP/6-31G* enthalpy of ΔH = - 14.9 kcal/mol for this reaction confirms that the difference between the secondary Si-H and P-H bond strengths is nearly the same between silacyclohexane and phosphacyclohexane as between dimethylsilane and dimethylphosphine.

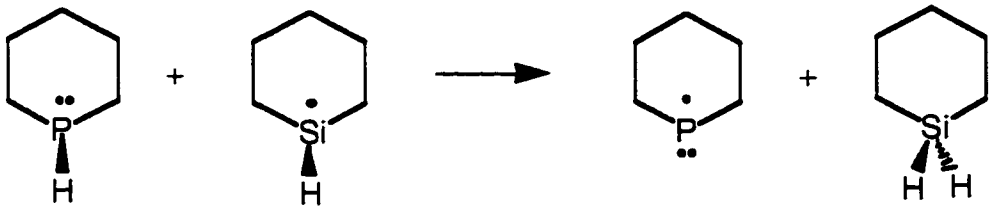

eq 12

As shown in Table 1, there is experimental evidence that, as predicted by B3LYP/6-31G*, G2,[8c] and other *ab initio*[27a] and DFT[27b] calculations, the Si-H BDE really does increase with increasing methyl substitution on silicon.[28,29] The increase in Si-H BDEs with increasing alkyl substitution can be attributed to the fact that, because silyl radical centers are pyramidal, hyperconjugative stabilization of silyl radicals is negligible. Since carbon is slightly more electronegative than hydrogen and since, in the absence of other effects, electronegative substituents tend to increase BDEs,[30] the small increase in Si-H BDEs with increasing alkyl substitution can be understood.[27a]

In contrast to the case with silyl radical centers, R_2P radical centers are divalent and, hence, necessarily planar. Consequently, phosphorus-centered radicals can be better stabilized by hyperconjugation than silyl-centered radicals. As shown in Table 1, alkyl groups are, in fact, computed to lower P-H BDEs. As also shown in Table 1, there is experimental evidence that, as predicted, P-H BDEs do decrease with increasing substitution on phosphorus.[31]

The increase in Si-H BDEs and the decrease in P-H BDEs with increasing alkyl substitution is responsible for the computational finding that the difference between the Si-H and P-H BDEs, given by the enthalpy of the isodesmic reaction in eq 12, is larger than the difference between the BDEs of H_3Si-H and H_2P-H. Nevertheless, the value of

ΔH = - 14.9 kcal/mol for the reaction in eq 12 is still 8.8 kcal/mol smaller in size than ΔH = - 23.7 kcal/mol for the isodesmic reaction in eq 11.

The compounds in these two equations differ in two obvious ways. First, the silyl radical center is planar in eq 11 but pyramidal in eq 12. Second, both radical centers in eq 11 are linearly conjugated to two double bonds, but these double bonds are absent in eq 12. By planarizing the silyl radical center in 1-silacyclohexyl, as in eq 13, the contribution of the former difference between eq 11 and eq 12 can be computed. The difference between the enthalpies of the isodesmic reactions in eq 11 and eq 13 then gives the contribution of the two double bonds to the enthalpy of the reaction in eq 11.

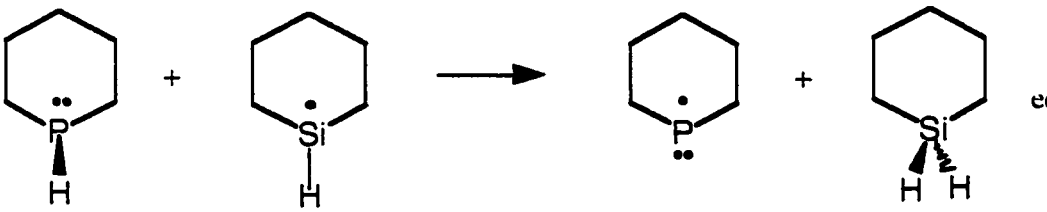

eq 13

Inversion of the silyl radical center is computed at the B3LYP/6-31G* level to require 8.8 kcal/mol in 1-silacyclohexyl, compared to 4.2 kcal/mol in 1-silacyclohexa-2,4-dienyl. The difference of 4.6 kcal/mol is the amount by which conjugation with the double bonds reduces the barrier to inversion of the silyl radical center in 1-silahexa-2,4-dienyl from that in 1-silacyclohexyl.

When the effect of the 8.8 kcal/mol increase in energy on planarization of the radical center in 1-silacyclohexyl is added to ΔH = - 14.9 kcal/mol for eq 12, eq 13 is computed to be exothermic by ΔH = - 23.7 kcal/mol. Thus, the enthalpy of the isodesmic

reaction in eq 13 is computed to be exactly the same as that for the isodesmic reaction in eq 11. This result shows that the presence of the two double bonds in the compounds in eq 11 has no effect on the *difference* between the Si-H and P-H BDEs that is given by the enthalpy of the isodesmic reaction in eq 13.

If the π conjugation energies of 1-phospha- and 1-silacyclohexa-2,4-diene are assumed to be the same in eq 11, the identical enthalpies of eq 11 and eq 13 imply that the π bonds formed to the planarized silyl radical center in 1-silacyclohexa-2,4-dienyl and to the phosphoryl radical center in 1-phospha-cyclohexa-2,4-dienyl have essentially the same strength. Comparison of the angles between the P-H bond and the C-P-C plane in 1-phosphacyclohexa-2,4-diene (78.2°) and in phosphacyclohexane (77.9°) indicates that there is little conjugation between the lone pair of electrons on phosphorus and the double bonds in 1-phosphacyclohexa-2,4-diene. Therefore, the π conjugation energies of 1-phospha- and 1-silacyclohexa-2,4-diene are, in fact, nearly the same.

It then follows from the identical enthalpies of eq 11 and eq 13 that the π systems of planar 1-silacyclohexa-2,4-dienyl and 1-phosphacyclohexa-2,4-dienyl do, indeed, have nearly the same energies. This conclusion, coupled with the near thermoneutrality of the reaction in eq 9 (ΔH = - 0.3 kcal/mol), implies that the delocalized π systems of **SB** and **PB** are also nearly isoenergetic.

Conclusions

In finding that the dimerization of **SB** is exothermic by ΔH = -21.5 kcal/mol and that of **PB** is endothermic by ΔH = 32.6 kcal/mol, the results of my B3LYP/6-31G*

calculations are consistent with the huge difference observed between the reactivity of these two compounds toward dimerization. The fact that the difference between the heats of dimerization is only about 11% larger than twice the calculated difference of 24.0 kcal/mol between the heats of hydrogen addition to **SB** and **PB**, indicates that the latter reaction can serve as a good model for the former.

I have used the difference between the addition of hydrogen to an Si-C π bond in **SB** and a P-C π bond in **PB** to try to understand the difference between the reactivity toward dimerization of these two heterobenzenes. My calculations reveal that the intrinsic strengths of the Si-C π bond in **SB** and the P-C π bond in **PB** are not very different. The difference of 4.5 kcal/mol, given by the enthalpy of the isodesmic reaction in eq 8, is less than 20% of the difference between the computed heats of hydrogen addition to **SB** and **PB**. The near thermoneutrality of eq 9, in which the the silyl radical in eq 8 is constrained to be planar, shows that the weaker π bond in **SB** can be attributed to the preference of the silyl radical for a pyramidal geometry.

These B3LYP/6-31G* calculations indicate that 19.5 kcal/mol of the difference between the enthalpies of the hydrogen addition reactions to **SB** and **PB** resides in the difference between the strengths of the Si-H and P-H bonds that are formed. Of this 19.5 kcal/mol, a little over half comes from the larger amount of 3s character in the bonds formed by tetravalent silicon than in the bonds formed by trivalent phosphorus. The 10.1 kcal/mol difference between the H_3Si-H and the H_2P-H B3LYP/6-31G* BDEs is attributed to this difference in hybridization.

A calculated contribution of an additional 4.8 kcal/mol to the difference between the strengths of the Si-H bond formed in the addition of hydrogen to **SB** and the P-H bond formed in the addition of hydrogen to **PB**, comes from the fact that alkyl substitution strengthens bonds to silicon but weakens bonds to phosphorus. Hyperconjugation provides less stabilization for silyl radicals, which are pyramidal, than for phosphoryl radicals, which are necessarily planar; and this effect acts to make the difference between Si-H and P-H BDEs increase with increasing alkyl substitution.

The source of the remaining 4.6 kcal mol difference between the strengths of the bonds formed at each of the heteroatoms in the addition of hydrogen to **SB** and **PB** is also related to the difference between the geometries of silyl and phosphoryl radicals. In order to fully planarize silicon in 1-silacyclohexyl radical, so that the radical center has the same type of geometry as that in 1-phosphacyclohexyl radical, 8.8 kcal mol is computed to be required. The finding that the isodesmic reaction in eq 13 is computed to have the same energy as the isodesmic reaction in eq 11, shows that, upon introduction of two double bonds into each of the six-membered rings, the planar radical centers give fully conjugated π systems with identical energies.

However, a planar geometry for 1-silacyclohexadienyl radical is not optimal. The equilibrium geometry, which has a pyramidal silyl radical center, is 4.2 kcal mol lower in energy. The difference between the 8.8 kcal mol that is required to planarize 1-silacyclohexyl radical and the 4.2 kcal mol that is released when planar 1-silacyclohexadienyl radical is allowed to pyramidalize is 4.6 kcal/mol. This is the third

contributor to the 19.5 kcal mol difference between the Si-H bond strength in 1-silacyclohexa-2,4-diene and the P-H bond strength in 1-phosphacyclohexa-2,4-diene.

An important general point is illustrated by the results of the calculations of the relative heats of hydrogen addition to **SB** and **PB**. Although it may be tempting to attribute a difference in reactivities between two compounds to the relative strengths of the bonds broken when each reacts, it is often the case that the major contributor is, instead, the relative strengths of the bonds that are formed.[32] From the results of these calculations on the addition of hydrogen to **SB** and **PB** I conclude that it is the difference in strengths between the bonds made to silicon in the dimerization **SB** and to phosphorus in the dimerization of **PB** which is chiefly responsible for making dimerization exothermic for **SB** but highly endothermic for **PB**.

Table 1. Calculated and Experimental Bond Dissociation Enthalpies (DH^{298}) in kcal mol.

Bond	B3LYP 6-31G*	G2	Experiment
H_3Si–H	90.0	92.7[a]	91.7[b]
$MeSiH_2$–H	90.6	93.7[c]	92.2[d]
Me_2SiH–H	91.4		
Me_3Si–H	92.1		95.1[e]
H_2P–H	79.9	82.9[f]	83.9,[b] 80.9[g]
MePH–H	78.1	81.9[h]	74.4 - 79.0[i]
Me_2P–H	76.8		

[a]Ref 3c gives DH^0 = 91.3 kcal mol. [b]From ref 24. [c]Ref 8c gives DH^0 = 92.3 kcal mol.[d]From ref 29b. [e]From ref 28. [f]Ref 8c gives DH^0 = 81.5 kcal mol. [g]From ref 25. [h]Ref 8c gives DH^0 = 80.5 kcal mol. [i]From ref 31.

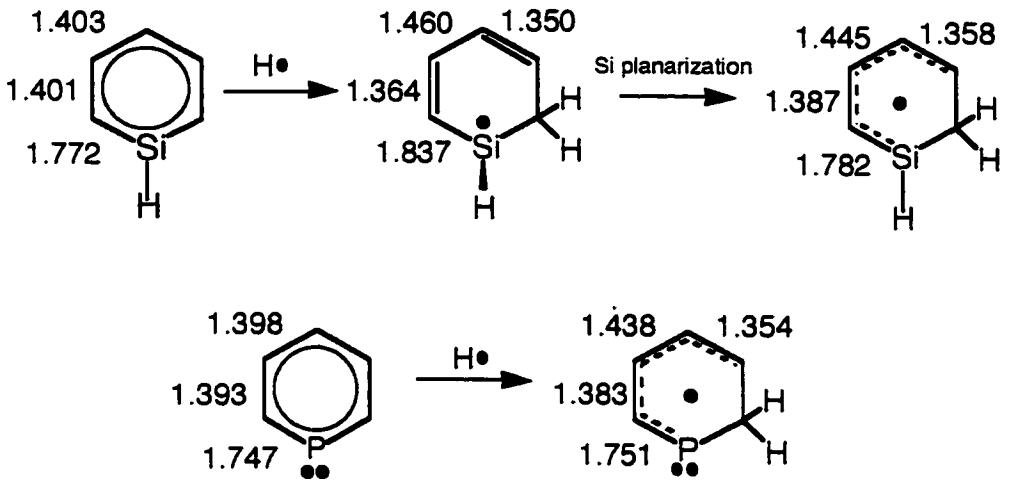

Figure 1. Changes in the B3LYP/6-31G* bond lengths that occur upon addition of a hydrogen atom to **SB** and **PB** and upon planarization of silicon in the radical formed from **SB.**

III. *Ab Initio* and Density Functional Theory Calculations on Heteroatom Analogues of Trimethylenemethane Radical Ions. Can a Quartet Be the Ground State?

Introduction

Since its conception by Moffitt[33] in 1948 and its synthesis and spectroscopic observation by Dowd[34] in 1966, trimethylenemethane (TMM) and its derivatives have become the most thoroughly studied non-Kekulé hydrocarbon diradicals.[35] The ground state of TMM has long been known to be a triplet,[34-36] as expected from both qualitative molecular orbital (MO)[37] and valence-bond (VB)[38] theories. The size of the singlet-triplet energy splitting has been measured[39] and found to be in good agreement with the results of high-level *ab initio* calculations.[40]

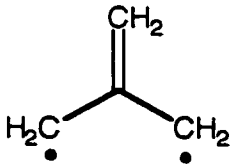

TMM

Much less is known about the radical ions of TMM than about the neutral diradical. The parent radical cation ($TMM^{\bullet+}$) has been generated by Shiotani and coworkers and studied by EPR.[41] As predicted computationally, ten years before the EPR study was performed,[42] the doublet ground state was found to pseudorotate from one Jahn-Teller-distorted geometry to another with little or no barrier. Derivatives of

$TMM^{\bullet+}$ have been formed as reactive intermediates by one-electron oxidation of methylenecyclopropanes.[43]

Even less is known about the TMM radical anion ($TMM^{\bullet-}$) than about the radical cation. $TMM^{\bullet-}$ was generated in the gas-phase by Hu and Squires and used to obtain the negative ion photoelectron spectrum of TMM.[39] In the same study, the results of CASSCF and UB3LYP calculations on the two, Jahn-Teller distorted, C_{2v} states of $TMM^{\bullet-}$ were reported. The $^2A_2$ state was computed to be 0.1 - 0.6 kcal mol lower in energy than the $^2B_1$ state.[39]

Recently, Iwamura and coworkers have prepared derivatives of TMM radical ions in which the three methylene groups were replaced by *p*-(*tert*-butylnitroxyl)phenyl groups and the central carbon was replaced by boron or by nitrogen.[44] $B(CH_2)_3^{\bullet}$ is isoelectronic with $TMM^{\bullet+}$, and $N(CH_2)_3^{\bullet}$ is isoelectronic with $TMM^{\bullet-}$.

EPR magnetic susceptibility studies showed that the $B(CH_2)_3^{\bullet}$ and $N(CH_2)_3^{\bullet}$ derivatives prepared by Iwamura and coworkers had doublet ground states. However, the presence of a thermally-populated, excited quartet state was detected in both compounds. UB3LYP calculations on a model for the aza compound, in which the *tert*-butyl substituents on the nitroxyl groups were replaced by methyls, gave a doublet-quartet energy separation that was in good agreement with that measured.[44]

Iwamura's study raises the question of whether it might be possible to prepare heteroatom analogues of TMM radical ions in which the ground state is a quartet, rather than a doublet. In this chapter, I address this question and report the results of *ab initio*

and density functional theory (DFT) calculations on the doublet-quartet energy differences (ΔE_{DQ}) in planar $X(CH_2)_3$ radicals with three π electrons (X = Al, B, and C^+) and five π electrons (X = C^-, N, O^+). I also describe how replacement of the three methylene groups in $Al(CH_2)_3^{\bullet}$ by oxygen atoms and in $O(CH_2)_3^{\bullet +}$ by SiH_2 groups affects the calculated values of ΔE_{DQ}.

I have found that the computational results on molecules containing three and five π electrons are mirrored by the results of calculations on $H_3^{\bullet}$ and $HeH_3^{\bullet}$ models. These models provide an explanation for why the quartet can fall below the doublet in properly designed heteroatom derivatives of $TMM^{\bullet -}$ but not in heteroatom derivatives of $TMM^{\bullet +}$.

Computational Methodology

Since I was interested in comparing the relative energies of the doublet and quartet states of the $X(CH_2)_3$ radicals with fully conjugated π systems, most of the calculations were performed on molecules that were constrained to be planar. The geometries of the doublet and quartet states of molecules, thus constrained, were optimized in the C_{2v} and D_{3h} point groups, respectively.

Especially for the $X(CH_2)_3$ radicals containing five π electrons, pyramidalization of X and or the peripheral CH_2 groups was computed to be energetically favorable. Consequently, for such molecules, the optimized C_{2v} and D_{3h} geometries are not energy minima but are stationary points of higher order, usually with several imaginary

vibrational frequencies. Therefore, the relative energies of the doublet and quartet states of such molecules were not corrected for differences between their zero-point vibrational energies. Unless otherwise specified, all calculations were performed with the 6-31+G(d) basis set.[15,45] Unrestricted (U)DFT calculations were carried out utilizing Becke's three-parameter, hybrid functional and the non-local correlation functional of Lee, Yang, and Parr (B3LYP).[16] The *Gaussian 98* suite of programs[46] was used to perform the UB3LYP calculations.

CASSCF calculations were carried out with the *GAMESS* package of *ab initio* programs.[47] The active space for the CASSCF calculations consisted of the number of π electrons in each species [e.g. three for $B(CH_2)_3^{\bullet}$ and five $N(CH_2)_3^{\bullet}$], distributed among the four π MOs of TMM. In order to include the effects of dynamic electron correlation[48] in the (3,4)CASSCF and (5,4)CASSCF calculations, CASPT2[49] single point calculations were performed at the CASSCF optimized geometries, using the *MOLCAS* suite of programs.[50]

Results and Discussion

Corrections for Artifactual Symmetry Breaking.

In the lowest doublet state of a planar $X(CH_2)_3$ radical that contains either three or five π electrons, an odd number of electrons must be placed in the pair of nonbonding π MOs. At D_{3h} geometries these MOs belong to the degenerate e″ representation of the

D_{3h} point group. Since the e_x'' and e_y'' NBMOs are degenerate at D_{3h} geometries, at such geometries the energies of the $^2E_x''$ and $^2E_y''$ states that result from singly occupying one or the other of these two NBMOs should be exactly the same.

However, in practice, the computed energies of the two states that result from singly occupying one or the other of the two NBMOs usually do not have exactly the same energy. As discussed in detail elsewhere,[42,51] approximate wave functions usually show artifactual symmetry breaking, because at D_{3h} geometries the two lowest doublet wave functions for $X(CH_2)_3$ radicals do not really have pure E_x'' and E_y'' symmetry. Instead the wave functions belong to, respectively the A_2 and B_1 representations of the C_{2v} subgroup of D_{3h}. Since A_2 and B_1 are not degenerate representations (the C_{2v} point group has none), at D_{3h} geometries the two lowest doublet wavefunctions generally do not have the same energy.

Like the pure $^2E_x''$ and $^2E_y''$ wavefunctions to which they correspond, the $^2A_2$ and $^2B_1$ states each undergo a first-order Jahn-Teller distortion[52] to a C_{2v} geometry of lower symmetry. One of these states is expected to represent the maxima and the other the minima along the lowest energy pathway for pseudorotation of the lowest doublet state of an $X(CH_2)_3$ radical around a D_{3h} geometry.[51] However, if the energies of these two states are spuriously computed to be different at D_{3h} geometries, there is every reason to believe that this energetic advantage of one state over another will also be manifested in the relative energies of the states at the optimized C_{2v} geometry of each.

The simplest way to correct for this effect of artifactual symmetry breaking, due to the approximate nature of the electronic wave functions, is to subtract the energy difference between $^2A_2$ and $^2B_1$ at a D_{3h} geometry (e.g., at the optimized geometry of the quartet, $^4A_1''$) from the energy difference between these two doublet states at the optimized C_{2v} geometry of each. For example, the calculations almost invariably found that, at the D_{3h} geometry of $^4A_1''$, $^2B_1$ was higher in energy than $^2A_2$. The energy that has to be subtracted from the energy of $^2B_1$, in order to make it degenerate with $^2A_2$ at the optimized D_{3h} geometry of $^4A_1''$ is shown in the first column of Table 2 and Table 3. The second column shows the energy of $^2B_1$, relative to $^2A_2$, at the optimized C_{2v} geometry of each state, after this correction for artifactual symmetry breaking has been applied.

The results in Table 2 and Table 3 show that artifactual symmetry breaking in $^2A_2$ and $^2B_1$ has a much larger effect on the relative UB3LYP energies of these two states than on their relative CASSCF or CASPT2 energies. The effect of artifactual symmetry breaking on theUB3LYP relative energies increases with the difference between the electronegativities of the central and terminal atoms.

As the difference between the electronegativities of the central and terminal atoms in XY_3 increases, configurations, other than the one of lowest energy, become increasingly important for both doublet states (*vide infra*). Since the UB3LYP calculations are based on wave functions that consist of a single configuration, it is not at

all surprising that, as the difference between the electronegativities of the central and terminal atoms in XY_3 increases, UB3LYP does a poorer job than CASSCF or CASPT2 of computing the relative energies of the two lowest doublet states.

Apparently, $^2B_1$, in which the unpaired electron occupies an orbital of the same symmetry (b_1) as the doubly-occupied π orbital(s), is less well-described by a single configuration at the UB3LYP level than is $^2A_2$, in which the unpaired electron occupies an orbital of different symmetry (a_2) than the doubly-occupied π orbital(s). The poorer quality of the UB3LYP wave functions for $^2B_1$, compared to those for $^2A_2$, is reflected, not only in the higher UB3LYP energies of $^2B_1$, relative to $^2A_2$, but also in the larger deviations of the values of $\langle S^2 \rangle$ for $^2B_1$ from the value of $\langle S^2 \rangle = 3/4$ for a pure doublet wave function. Therefore, in discussing the UB3LYP results in Table 2 and Table 3, I shall use the $^2A_2$, rather than the $^2B_1$ energies.

As the quality of the wave functions for the components of a degenerate state improves, the amount of artifactual symmetry breaking decreases, and the energies of the components become more nearly the same at the geometry of highest symmetry. This can be clearly seen by comparing the sizes of the CASSCF and CASPT2 corrections for artifactual symmetry breaking in Table 2 and Table 3 with the UB3LYP corrections. Except in $C(CH_2)_3^{\bullet -}$, the largest CASSCF correction is 0.3 kcal/mol, and the largest CASPT2 correction is 0.1 kcal/mol.

Effect of Including Dynamic Electron Correlation.

The (3,4)- and (5,4)CASSCF calculations do not include the effects of dynamic electron correlation between the σ and the π electrons,[48] but the CASPT2 calculations do. Therefore, there is every reason to expect the CASPT2 results for $E(^4A_1'') - E(^2A_2)$ $= \Delta E_{DQ}$ in Table 2 and Table 3 to be more accurate than the CASSCF results.

UB3LYP does not explicitly include any correlation between the σ and the π electrons in the Kohn-Sham orbitals from which the densities are computed. However, the effects of both dynamic and non-dynamic electron correlation are included in the B3LYP functional, from which the energy is calculated.

Thus, perhaps it is not surprising that inspection of Table 2 and Table 3 shows the energy differences between $^4A_1''$ and $^2A_2$, obtained by the CASPT2 and UB3LYP calculations, are generally in much better agreement with each other than with the CASSCF results. Consequently the following discussions of ΔE_{DQ} for the molecules in Table 2 and Table 3 is based on the CASPT2 and UB3LYP results for the energy differences between $^4A_1''$ and $^2A_2$ in Table 2 and Table 3, rather than on the CASSCF results.

Effect of Heteroatom Substitution on ΔE_{DQ} in $C(CH_2)^{\cdot+}$.

The values of ΔE_{DQ} in Table 2 for the $X(CH_2)_2$ radicals with three π electrons decrease in the order, $X = C^+ > X = B > X = Al$. The reasons for this decrease are easy to

understand from the $X(CH_2)_3$ π MOs and how they are occupied in the lowest doublet and quartet states. The MOs and their occupancies in $^2A_2$ and $^4A_1''$ are depicted schematically in Figure 2.

The formation of $^4A_1''$ from either of the lowest doublet states requires the excitation of an electron from the bonding $1a_2''$ MO to the e'' NBMO that is empty. Therefore, the difference between the e'' and $1a_2''$ orbital energies plays a crucial role in determining the size of ΔE_{DQ} for the radicals in Table 2. Since $1a_2''$ is a bonding MO and e'' is non-bonding, ΔE_{DQ} should decrease with a decrease in the strength of the π bonds between the central atom, X, and CH_2. Thus, since π bond strengths decrease in the order π(C-C) > π(B-C) > π (Al-C),[53] the fact that ΔE_{DQ} decreases in the same order is easily understandable.

However, this is not the only manner in which the identity of X in $X(CH_2)_3$ affects the difference between the e'' and $1a_2''$ orbital energies and, hence, the size of ΔE_{DQ}. As shown in Figure 2, the e'' MOs have a node at the central atom; whereas, $1a_2''$ does not. Consequently, an $1a_2'' \rightarrow e''$ excitation transfers electron density from X to the peripheral carbons. Thus, the less electronegative X is, relative to C, the smaller the $e'' - 1a_2''$ orbital energy difference and the lower the calculated size of the ΔE_{DQ} energy difference in Table 2.

Replacing $Y = CH_2$ in XY_3 with a more electronegative group or atom should also decrease the size of the $e'' - 1a_2''$ orbital energy difference and, hence, the size of

ΔE_{DQ}. As shown in Table 2, going from $Al(CH_2)_3$ to AlO_3 is computed to lower the CASPT2 value of ΔE_{DQ} from 4.4 kcal/mol to only 1.0 kcal/mol. Since an Al-O π bond is stronger than an Al-C π bond,[53] this decrease in ΔE_{DQ} is clearly not due to a decrease in π bond strengths but to the greater electronegativity of O, relative to CH_2.

A Simple Model for XY_3 Radicals with Three π Electrons and Y Much More Electronegative than X.

In a hypothetical XY_3 radical that is isoelectronic with $C(CH_2)_3^{\cdot +}$, if Y were *infinitely* more electronegative than X, all three π electrons would be localized in p-π AOs on the electronegative Y atoms. If there really were no delocalization of electrons into the empty p-π AO on X, this would be equivalent to not having a p-π AO on the central atom or to not having a central atom at all. Therefore, $H_3^{\cdot}$ with equal separations between all three hydrogens should provide an adequate model for the π system of such an XY_3 radical at D_{3h} geometries.[54]

Correlation between the three electrons in the three 1s orbitals of $H_3^{\cdot}$ can be handled by (3 3)CASSCF calculations. The results of (3 3)CASSCF/6-311G(p) calculations on $H_3^{\cdot}$ at D_{3h} geometries are given in Table 4. The Table shows that, as the distance, R, between the three hydrogen atoms and their collective center of mass decreases, the energy of the $^4A_2'$ state rises monotonically, while that of the $^2E'$ state decreases by 20.9 kcal/mol between $R = 4.00$ Å and the D_{3h} minimum at $R = 0.65$ Å.

Consequently, although the energies of $^4A_2'$ and $^2E'$ are essentially the same at R = 4.0 Å, the energy of $^4A_2'$ never falls below that of $^2E'$. Jahn-Teller distortions of $^2E'$ from D_{3h} geometries would, of course, further stabilize the doublet state.[54]

The results in Table 4 of the CASSCF calculations on the $H_3^{\bullet}$ model indicate that a doublet should also be the ground state of an XY_3 radical, containing three π electrons, even if Y were infinitely more electronegative than X. In order to understand why a doublet is expected to be the ground state, even under those circumstances most likely to provide the smallest values of ΔE_{DQ}, it is instructive to continue to exploit the simple $H_3^{\bullet}$ model.

Placing one electron in each 1s AO (ϕ) of $H_3^{\bullet}$ minimizes the coulombic repulsion energy between electrons. For the $^4A_2'$ state this distribution of the three electrons is, of course, the only one allowed by the Pauli exclusion principle. eq 14 gives the wave function for the component of the quartet in which the electron in each AO has spin α.

$$^4\Psi = |\phi_1^{\alpha}\phi_2^{\alpha}\phi_3^{\alpha}\rangle \qquad \text{eq 14}$$

However, the quartet is not the only state in which one electron can be localized in each 1s AO of $H_3^{\bullet}$. There is a $^2E'$ state in which this is also possible. The wave

functions for its two components, $^2E_x'$ and $^2E_y'$ (respectively, $^2A_1$ and $^2B_1$ in C_{2v} symmetry), are given in eq 15 and eq 16.

$$^2\Psi_x = \frac{1}{\sqrt{6}}\left[2\left|\varphi_1^\beta\varphi_2^\alpha\varphi_3^\alpha\right\rangle - \left|\varphi_1^\alpha\varphi_2^\beta\varphi_3^\alpha\right\rangle - \left|\varphi_1^\alpha\varphi_2^\alpha\varphi_3^\beta\right\rangle\right] \qquad \text{eq 15}$$

$$^2\Psi_y = \frac{1}{\sqrt{2}}\left[\left|\varphi_1^\alpha\varphi_2^\beta\varphi_3^\alpha\right\rangle - \left|\varphi_1^\alpha\varphi_2^\alpha\varphi_3^\beta\right\rangle\right] \qquad \text{eq 16}$$

It is possible to rewrite the valence-bond wave functions in eq 14, eq 15, and eq 16 in terms of MOs. The normalized MOs, ψ, of D_{3h} H_3^* can be expressed as linear combinations of the 1s AOs. eq 17 gives the wave function for the a_1 MO (ψ_1); and eq 18 and eq 19 give, respectively, the wave functions for the degenerate pair of e_x (ψ_2) and e_y (ψ_3) MOs. The normalizations assume that the overlap between AOs is either negligible or is small enough to be neglected.

$$\psi_1 = \frac{1}{\sqrt{3}}(\varphi_1 + \varphi_2 + \varphi_3) \qquad \text{eq 17}$$

$$\psi_2 = \frac{1}{\sqrt{2}}(\varphi_2 - \varphi_3) \qquad \text{eq 18}$$

$$\psi_3 = \frac{1}{\sqrt{6}}(2\varphi_1 - \varphi_2 - \varphi_3) \qquad \text{eq 19}$$

Using eq 17, eq 18, and eq 19, each of the AOs can each be written as a linear combination of the MOs. Solving eq 17, eq 18, and eq 19 for each of the AOs affords

$$\varphi_1 = \frac{\sqrt{3}}{3}\psi_1 + \frac{\sqrt{6}}{3}\psi_3 \qquad \text{eq 20}$$

$$\varphi_2 = \frac{\sqrt{3}}{3}\psi_1 + \frac{\sqrt{2}}{2}\psi_2 - \frac{\sqrt{6}}{6}\psi_3 \qquad \text{eq 21}$$

$$\varphi_3 = \frac{\sqrt{3}}{3}\psi_1 - \frac{\sqrt{2}}{2}\psi_2 - \frac{\sqrt{6}}{6}\psi_3 \qquad \text{eq 22}$$

Substituting eq 20, eq 21, and eq 22 into eq 14 gives the $^4A_2'$ wavefunction, expressed in terms of MOs. Not surprisingly, it reduces to the wave function in eq 23, which places one α electron in each MO.

$$^4\Psi = \left|\psi_1^{\alpha}\psi_2^{\alpha}\psi_3^{\alpha}\right\rangle \qquad \text{eq 23}$$

Using eq 20, eq 21, and eq 22, the $^2E'$ wave functions in eqs 2 and 3 can also be expressed in terms of the MOs in eq 17, eq 18, and eq 19. However, unlike the $^4A_2'$ wavefunction in eq 23, the $^2E'$ wave functions turn out to be linear combinations of

configurations, each of which assigns the three electrons to a different set of MOs. The $^2E_x'$ wave function is given in eq 24, and the $^2E_y'$ wave function is given in eq 25.

$$^2\Psi_x = \frac{1}{\sqrt{3}}\left[\left|\psi_1^2\psi_2^\alpha\right\rangle - \left|\psi_2^\alpha\psi_3^2\right\rangle - \frac{1}{\sqrt{2}}\left(\left|\psi_1^\alpha\psi_2^\alpha\psi_3^\beta\right\rangle - \left|\psi_1^\alpha\psi_2^\beta\psi_3^\alpha\right\rangle\right)\right] \qquad \text{eq 24}$$

$$^2\Psi_y = \frac{1}{\sqrt{3}}\left[\left|\psi_1^2\psi_3^\alpha\right\rangle - \left|\psi_2^2\psi_3^\alpha\right\rangle - \frac{1}{\sqrt{2}}\left(\left|\psi_1^\alpha\psi_2^2\right\rangle - \left|\psi_1^\alpha\psi_3^2\right\rangle\right)\right] \qquad \text{eq 25}$$

At sufficiently large H–H distances, the quartet wave function in eq 23 has exactly the same energy as the degenerate doublet wave functions in eq 24 and eq 25. However, as the hydrogen 1s AOs begin to overlap, two effects alter the relative energies of $^4A_2'$ and $^2E'$. One involves electron repulsion in the overlap regions between the hydrogen atoms, which selectively stabilizes the quartet. The other involves bonding between the hydrogens, which selectively stabilizes the doublet.

The quartet wave function not only keeps the electrons from appearing in the same AO, but $^4\Psi$ also prevents the electrons from appearing simultaneously in the regions where two of the 1s AOs overlap. The doublet wave functions, $^2\Psi_x$ and $^2\Psi_y$, contain one electron that has opposite spin from the other two, and there is no prohibition against having a pair of electrons of opposite spin simultaneously in the same overlap region.[55] Consequently, the doublet wave functions each have a slightly higher coulombic repulsion energy than the quartet, when the hydrogen 1s AOs begin to overlap.

On the other hand, in the quartet the interactions between the hydrogen atoms are all antibonding; but in the doublets some are bonding and some are antibonding. For example, using eq 15, it is easy to show that in $^2\Psi_x$ the interactions between ϕ_1 and both ϕ_2 and ϕ_3 are weakly bonding, but the interaction between ϕ_2 and ϕ_3 is antibonding. Similarly, using eq 16 it can be shown that just the reverse is true in $^2\Psi_y$; the interactions between ϕ_1 and both ϕ_2 and ϕ_3 are weakly antibonding, but the interaction between ϕ_2 and ϕ_3 is bonding. Overall, the doublet wave functions are each nonbonding. However, the quartet wave function is antibonding between all the hydrogens, and this confers an energetic advantage on the doublet.

The CASSCF calculations find that, as the AOs of H_3 begin to overlap, if the weights of the three types of configurations in each of the doublet wave functions in eq 24 and eq 25 are kept equal, the quartet falls below the doublets in energy.[56] However, as the AOs begin to overlap, and ψ_1 is stabilized, relative to ψ_2 and ψ_3, the coefficients of the three types of configurations in eq 24 and eq 25 do not remain equal. For example, in eq 26 for the $^2E_x'$ wave function, c_1, the coefficient of the configuration in which ψ_1 is doubly occupied, increases; and c_2, the coefficient of the configuration in which ψ_1 is empty decreases, as does the coefficient of the pair of configurations in which ψ_1 is singly occupied. The resulting increase in bonding between the hydrogens is what causes the doublets to be stabilized as the 1s AOs of the hydrogens begin to overlap.

$$^2\Psi_x = c_1\left|\psi_1^2\psi_2^\alpha\right\rangle - c_2\left|\psi_2^\alpha\psi_3^2\right\rangle - \frac{c_3}{\sqrt{2}}\left(\left|\psi_1^\alpha\psi_2^\alpha\psi_3^\beta\right\rangle - \left|\psi_1^\alpha\psi_2^\beta\psi_3^\alpha\right\rangle\right) \qquad \text{eq 26}$$

Table 4 gives the coefficients of the three configurations in the $^2\Psi_x$ wave function for H_3 at several distances, R, between each of the hydrogens and their center of mass. The degeneracy of $^2E_x'$ and $^2E_y'$ at D_{3h} geometries ensures that, as the hydrogens begin to overlap, the changes in the coefficients of the configurations in $^2\Psi_y$ are the same as those in the coefficients of the corresponding configurations in eq 26 for $^2\Psi_x$. Table 4 shows the changes in the coefficients of the configurations in the $^2E'$ wave functions are accompanied by a decrease in energy of this state by 20.9 kcal mol on going from R = 4.00 Å to the D_{3h} geometry of minimum energy at R = 0.65 Å.

Bonding between the hydrogen 1s AOs favors the doublet state over the quartet in the H_3 model for an XY_3 radical that contains three π electrons and in which Y is much more electronegative than X. Similarly, even if π bonding between X and Y does not provide any stabilization for the doublet state in such an XY_3 radical, bonding between the 2p-π AOs on Y will result in a doublet ground state. Consequently, I predict it is highly unlikely that an XY_3 radical, containing three π electrons, will ever be found in which the quartet is the ground state.

Effect of Heteroatom Substitution on ΔE_{DQ} in $C(CH_2)_3^{\bullet -}$.

For $X(CH_2)_3$ molecules with five π electrons, ΔE_{DQ} in Table 3 shows exactly the opposite trend from ΔE_{DQ} in Table 2 for $X(CH_2)_3$ molecules with three π electrons. The value of ΔE_{DQ} in Table 3 decreases with increasing electronegativity of X in the order X ($C^- > N > O^+$). Figure 3 shows that this decrease cannot be due to the fact that π bond strengths increase in the order π(C=C) < π(N=C) < π (O=C),[53] since formation of $^4A_1''$ from either of the lowest doublet states requires the excitation of an electron from the doubly-occupied e'' NBMOs to the antibonding $2a_2''$ MO. This excitation energy, and, hence, the size of ΔE_{DQ}, should increase with the strength of a π bond between X and CH_2; but the trend in Table 3 is just the opposite.

Instead, the decrease in ΔE_{DQ} with the electronegativity of X is due the fact that an $e'' \rightarrow 2a_2''$ excitation transfers electron density from CH_2 to X. As already noted, e'' has a node at the central atom, X; whereas $2a_2''$, like $1a_2''$, does not. Therefore, the $e'' \rightarrow 2a_2''$ excitation energy behaves exactly opposite to the $1a_2'' \rightarrow e''$ excitation energy and decreases with increasing electronegativity of X, relative to CH_2.

On going from X = C^- to X = N in $X(CH_2)_3$, the calculated decrease in ΔE_{DQ} is rather small. The decrease is calculated to be only 4.9 kcal/mol by CASPT2 and 1.8 kcal/mol by UB3LYP. However, the extra electron in $^2A_2$ $C(CH_2)_3^{\bullet -}$ is computed to be unbound (EA= -6.7 kcal/mol) by CASPT2 and barely bound (EA= 5.3 kcal/mol) by UB3LYP.[57] Since $\Delta E_{DQ} > 40$ kcal/mol at both levels of theory, in the $^4A_1''$ state of the

radical anion the electron in the $2a_2''$ MO is unbound by ca. 50 kcal/mol at the CASPT2 level and by ca. 35 kcal/mol at UB3LYP.

Hence, in the $^4A_1''$ state of $C(CH_2)_3^{\cdot -}$ the electron in the $2a_2''$ MO occupies a very diffuse, Rydberg-like, orbital, rather than a valence orbital, as in $N(CH_2)_3\cdot$. Therefore, the difference between the values of ΔE_{DQ} in $C(CH_2)_3^{\cdot -}$ and $N(CH_2)_3\cdot$ does not really reflect the difference between the energies of the $2a_2''$ valence orbitals in these two radicals.

In the $^4A_1''$ states of both $N(CH_2)_3\cdot$ and $O(CH_2)_3^{\cdot +}$, $2a_2''$ is a valence orbital. As a result, comparison of the ΔE_{DQ} values in $N(CH_2)_3\cdot$ and $O(CH_2)_3^{\cdot +}$ does reflect the effect of the difference between the electronegativities of N and O on the relative energies of the $2a_2''$ MOs. It is for this reason that ΔE_{DQ} decreases by ca. 30 kcal/mol on going from $N(CH_2)_3\cdot$ to $O(CH_2)_3^{\cdot +}$.

Replacing N by a more electronegative atom is one way to decrease the $e'' \rightarrow 2a_2''$ excitation energy and, hence, the size of ΔE_{DQ}. Another way is to replace carbon in CH_2 by a more electropositive element, such as Si. The substitution of SiH_2 for CH_2 lowers the $e'' \rightarrow 2a_2''$ excitation energy not only because Si is less electronegative than C, but also by virtue of the fact that a π bond to Si is weaker than a π bond to C.[23]

As shown in Table 3, the CASPT2 value of $\Delta E_{DQ} = 9.0$ kcal/mol for $O(CH_2)_3^{\cdot +}$ decreases to -0.8 kcal/mol for $O(SiH_2)_3^{\cdot +}$. Thus, in planar $O(SiH_2)_3^{\cdot +}$ the quartet is actually predicted to fall slightly below the doublet in energy.[58]

A Simple Model for XY_3 Radicals with Five π Electrons and X Much More Electronegative than Y.

Why is it possible to find a planar XY_3 radical with a quartet ground state when there are five π electrons, but not when there are three π electrons? As already discussed, an H_3• model predicts that the doublet will always remain the ground state of XY_3• when there are three π electrons, no matter how much more electronegative Y is than X. Therefore, it is reasonable to ask if a similarly simple model predicts that the quartet can become the ground state of XY_3• when there are five π electrons and X is much more electronegative than Y.

In the model for the five-electron case I again used three hydrogen atoms, arranged in the geometry of an equilateral triangle, as Y in XY_3•. As a very electronegative central atom with two valence electrons I chose He. I then carried out (5,4)CASSCF/6-311G(p) calculations on HeH_3• at D_{3h} geometries with different values of the He-H distance, *R*. The results are summarized in Table 5.

As shown in this Table, as *R* is decreased, the energies of both the $^2E'$ and $^4A_2'$ states of HeH_3• increase monotonically. At small *R* $^2E'$ is the ground state. However, at intermediate values of *R*, the quartet falls below the doublet. Thus, at these values of *R*, the HeH_3• model successfully reproduces what the CASSCF and CASPT2 calculations predict to occur in planar $O(SiH_2)_3^{\bullet+}$ — the quartet becomes the ground state.

In understanding why the quartet falls below the doublet in both $O(SiH_2)_3^{\cdot+}$ and in the $HeH_3^{\cdot}$ model for it, eq 27, is useful. It gives the wave function for the $^2E_x'$ component of $^2E'$ in $HeH_3^{\cdot}$. eq 27 differs from eq 26 by the fact that each configuration in eq 27 contains a term, He^2, for the two electrons that occupy the 1s AO on helium. However, as in eq 26, ψ_1, ψ_2, and ψ_3 are the combinations of hydrogen defined by eq 17, eq 18, and eq 19.

$$^2\Psi_x = c_1\left|He^2\psi_1^2\psi_2^\alpha\right\rangle - c_2\left|He^2\psi_2^\alpha\psi_3^2\right\rangle - \frac{c_3}{\sqrt{2}}\left(\left|He^2\psi_1^\alpha\psi_2^\alpha\psi_3^\beta\right\rangle - \left|He^2\psi_1^\alpha\psi_2^\beta\psi_3^\alpha\right\rangle\right) \qquad \text{eq 27}$$

In $HeH_3^{\cdot}$, ψ_2 and ψ_3 each have a node at the He atom, but ψ_1 has the correct symmetry to interact with the He 1s AO. Since ψ_1 interacts with this doubly-occupied orbital of much lower energy, ψ_1 is destabilized by this interaction.

Table 5 shows how the coefficients of the configurations in the $^2E'$ wave functions change as the He-H distance, R, decreases and the interaction between ψ_1 and the He 1s AO increases. Since ψ_1 is destabilized by its interaction with the He 1s AO, at values of $R < 2.5$ Å the coefficient, c_2, of the configuration in which ψ_1 is empty increases at the expense of c_1, the coefficient of the configuration in which ψ_1 is doubly occupied. As R decreases, c_3, the coefficient of the configurations in which ψ_1 is singly occupied also decreases, but to a much lesser extent than does c_1.

Nevertheless, at He-H distances, where the increases in the energies of both $^2E'$ and $^4A_2'$ show that there is a non-negligible interaction between the 1s orbitals of these atoms (e.g., at R = 2.0 Å), the coefficients c_1, c_2, and c_3 remain nearly equal. The reason is that, as the He-H distance decreases, the H-H distances also decrease. Although the He-H interactions in ψ_1 are antibonding in $HeH_3^{\bullet}$, the H-H interactions in ψ_1 are bonding in $HeH_3^{\bullet}$, as they are in $H_3^{\bullet}$. These two opposing effects on the energy of ψ_1 are what tend to keep the coefficients c_1, c_2, and c_3 nearly equal, until values of R are reached at which He-H antibonding dominates H-H bonding (e.g. at R = 1.0 Å).

As already discussed, when these coefficients are equal or nearly so, the quartet has the advantage of having a slightly lower Coulombic repulsion energy than the doublet, because the Pauli principle prevents electrons of the same spin from simultaneously appearing in the overlap regions between atoms. Thus, at geometries of $HeH_3^{\bullet}$ where an appreciable fraction of the He-H antibonding interactions in the doublet are canceled by H-H bonding interactions, the lower Coulombic repulsion in the quartet can become the dominant effect and cause $^4A_2'$ to fall below $^2E'$.

Comparison of the CASSCF coefficients for the configurations in the $^2E'$ wave functions in Table 4 and Table 5 shows that, at the same values of R (e.g., R = 1.5 Å), c_1 and c_2 are more nearly equal in $HeH_3^{\bullet}$ than in $H_3^{\bullet}$. Similarly, one would expect the CASSCF coefficients for the configurations in the $^2A_2$ wave functions that correspond to the first two configurations in eq 26 and eq 27 to be more nearly equal in $O(SiH_2)_3^{\bullet+}$

than in AlO_3·. In fact, at the equilibrium geometries of the doublet states of these two radicals, $(c_2 \quad c_1)^2 = 1.12$ in $O(SiH_2)_3{}^{\cdot +}$, but $(c_1 \quad c_2)^2 = 1.23$ in $AlO_3{}^{\cdot}$.[59]

Conclusions

The CASSCF, CASPT2, and UB3LYP calculations all predict $AlO_3{}^{\cdot}$ to have a doublet ground state; whereas, the same types of calculations all predict the ground state of $O(SiH_2)_3{}^{\cdot +}$ to be a quartet. Model calculations on $H_3{}^{\cdot}$ and $HeH_3{}^{\cdot}$ support the following explanation for this difference between $AlO_3{}^{\cdot}$ and $O(SiH_2)_3{}^{\cdot +}$.

In $AlO_3{}^{\cdot}$ the Al-O and the O-O π interactions both selectively stabilize the $1a_2''$ bonding MO and, hence, favor the doublet state over the quartet. In contrast, in $O(SiH_2)_3{}^{\cdot +}$ destabilization by O-Si π antibonding of the $2a_2''$ MO that is largely localized on the silicons is partially offset by Si-Si π bonding. As a result, occupancy of this π MO is not strongly disfavored, relative to occupancy of an e' non-bonding MO. Consequently, in $O(SiH_2)_3{}^{\cdot +}$ the lower electron repulsion in the quartet can overcome the only slightly larger amount of π bonding in the doublet.

More generally, the results described in this chapter predict that the ground state of an XY_3 radical with three π electrons will always be a doublet, even if Y is much more electronegative than X. In contrast, in an XY_3 radical with five π electrons, if X is much more electronegative than Y, there is at least a possibility that the ground state will be a quartet.

I hope that the predictions of how ΔE_{DQ} depends on the electronegativities of X and Y in XY_3 radicals with three and with five π electrons will be useful in designing XY_3 radicals with very low-lying excited quartet states. I also hope these predictions – that the doublet will be the ground state of every XY_3 radical with three π electrons, but that the quartet can become the ground state of a planar XY_3 radical with five π electrons, when X is much more electronegative than Y – will stimulate experimental tests.

Table 2. Relative Energies (kcal/mol), Calculated for the Electronic States in XY_3 Radicals Containing Three π Electrons.

Molecule	Method	$E(^2B_1) - E(^2A_2)^a$	$E(^2B_1)^{corr} - E(^2A_2)^b$	$E(^4A_1'') - E(^2A_2)^c$
$C(CH_2)_3^{\cdot+}$	CASSCF	0.3	0.2	56.1
	CASPT2	0.1	-0.2	62.7
	B3LYP	2.0	-0.3	63.0
$B(CH_2)_3$	CASSCF	0.0	0.0	17.2
	CASPT2	0.0	-0.1	23.3
	B3LYP	6.9	-2.3	23.7
$Al(CH_2)_3$	CASSCF	0.1	-0.2	2.7
	CASPT2	0.0	0.0	4.4
	B3LYP	18.7	0.4	4.5
NO_3	CASSCF	0.0	0.0	0.4
	CASPT2	0.0	0.0	1.0
	B3LYP	48.5	-1.8	0.9

[a]Energy, which, when subtracted from that of $^2B_1$, would make the energy of $^2B_1$ the same as that of $^2A_2$ at the D_{3h} equilibrium geometry of $^4A_1''$. [b]Relative energies of $^2B_1$ and $^2A_2$ at their equilibrium geometries, after correction of the energy of $^2B_1$ for the effect of artifactual symmetry breaking at the D_{3h} geometry of $^4A_1''$. [c]ΔE_{DQ}.

Table 3. Relative Energies (kcal/mol), Calculated for the Electronic States in XY_3 Radicals Containing Five π Electrons.

Molecule	Method	$E(^2B_1) - E(^2A_2)^a$	$E(^2B_1)^{corr} - E(^2A_2)^b$	$E(^4A_1'') - E(^2A_2)^c$
$C(CH_2)_3^{\cdot -}$	CASSCF	1.2	-1.1	49.2
	CASPT2	-0.9	0.6	42.9
	B3LYP	0.2	0.2	40.5
$N(CH_2)_3$	CASSCF	-0.2	-0.6	32.5
	CASPT2	0.1	0.3	38.0
	B3LYP	2.3	-0.7	38.0
$O(CH_2)_3^{\cdot +}$	CASSCF	0.0	-0.1	5.1
	CASPT2	0.0	-0.1	8.9
	B3LYP	17.7	-4.1	8.0
$O(SiH_2)_3^{\cdot +}$	CASSCF	0.0	0.0	-0.9
	CASPT2	0.0	0.0	-0.8
	B3LYP	22.1	0.0	-0.1

[a]Energy, which, when subtracted from that of $^2B_1$, would make the energy of $^2B_1$ the same as that of $^2A_2$ at the D_{3h} equilibrium geometry of $^4A_1''$. [b]Relative energies of $^2B_1$ and $^2A_2$ at their equilibrium geometries, after correction of the energy of $^2B_1$ for the effect of artifactual symmetry breaking at the D_{3h} geometry of $^4A_1''$. [c]ΔE_{DQ}.

Table 4. (3,3)CASSCF/6-311G(p) Energies (kcal/mol) and Coefficients of the Configurations in the Wave Function (Eq. 13) for the $^2E'$ state of D_{3h} H_3 as a Function of the Distance, R, from the Center of Mass. Energies Are Relative to the D_{3h} Minimum for $^2E'$ at $R = 0.65$ Å.

R (Å)	c_1	c_2	c_3	$E(^2E')$	$E(^4A_2')$	ΔE_{DQ}
0.65	0.975	0.134	0.181	0[a]	158.24	158.24
1.0	0.859	0.286	0.427	12.47	52.74	40.27
1.5	0.683	0.471	0.559	20.06	24.26	4.2
2.0	0.608	0.546	0.576	20.86	21.18	0.32
2.5	0.585	0.569	0.577	20.91	20.91	0.0
3.0	0.579	0.575	0.577	20.92	20.92	0.0

[a] $E = -1.532765$ hartrees.

Table 5. (3/3)CASSCF/6-311G(p) Energies (kcal/mol) and Coefficients of the Configurations in the Wave Function (Eq. 14) for the $^2E'$ state of D_{3h} HeH_3^+ as a Function of the He-H Distance, R. Energies Are Relative to that of $^2E'$ at $R = 4.0$ Å.

R (Å)	c_1	c_2	c_3	$E(^2E')$	$E(^4A_2')$	ΔE_{DQ}
1.0	0.355	0.794	0.489	148.55	158.83	-10.27
1.5	0.538	0.615	0.575	37.35	37.19	0.16[a]
2.0	0.575	0.580	0.577	7.92	7.85	0.07
2.5	0.579	0.576	0.577	1.48	1.47	0.01
3.0	0.578	0.577	0.577	0.24	0.24	0.00
4.0	0.577	0.577	0.577	0[b]	0.00	0.00

[a] The maximum value of $\Delta E_{DQ} = 0.23$ kcal/mol was found to occur around $R = 1.6$ Å. [b] E = -4.359325 hartrees.

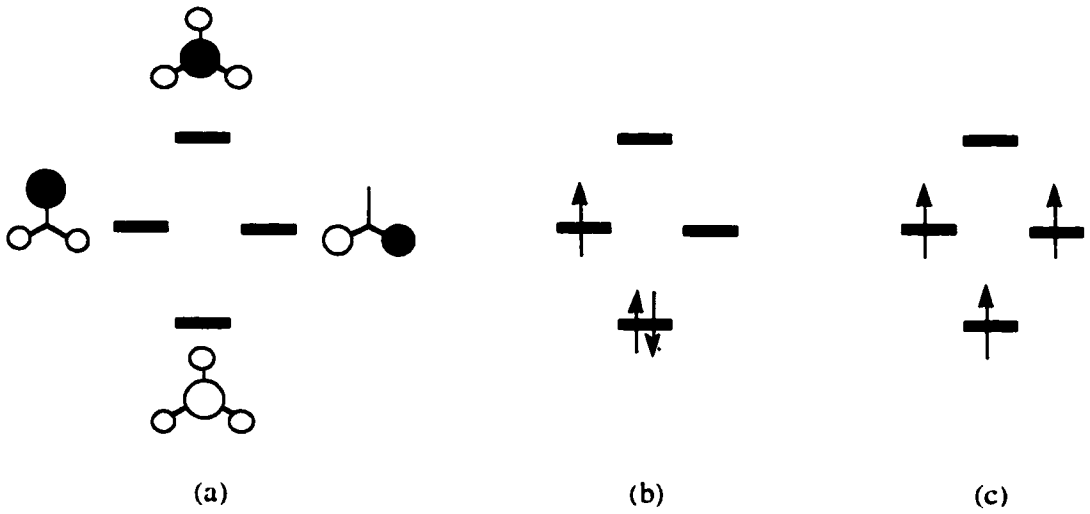

Figure 2. Schematic depiction of (a) the π MOs for TMM and how they are occupied in the (b) $^2E_y''$ and (c) $^4A_1''$ states of an XY_3 radical containing three π electrons.

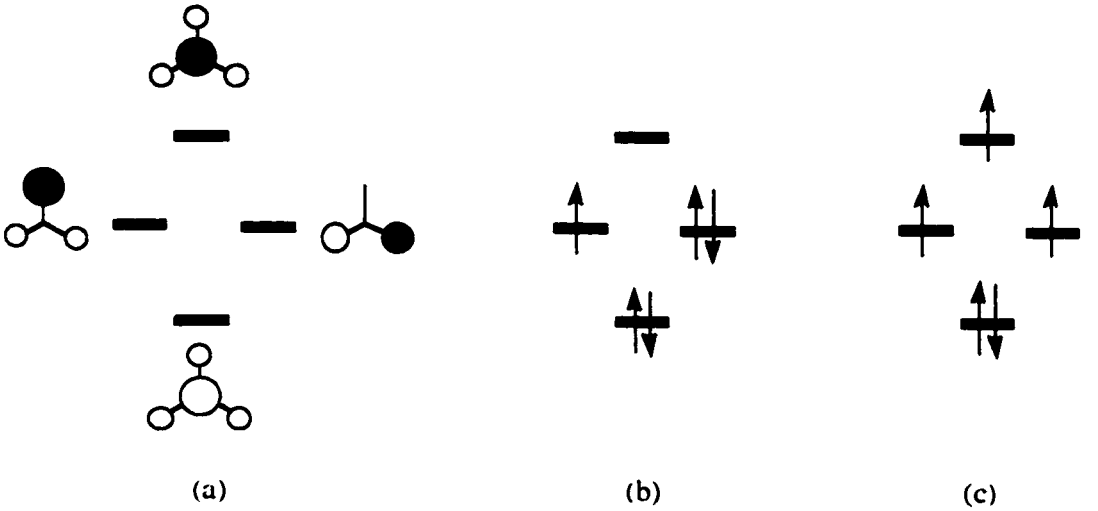

Figure 3. Schematic depiction of (a) the π MOs for TMM and how they are occupied in the (b) $^2E_y''$ and (c) $^4A_1''$ states of an XY_3 radical containing five π electrons.

IV. Are 1,5-Disubstituted Semibullvalenes that Have C_{2v} Equilibrium Geometries Necessarily Bishomoaromatic?

Introduction

Semibullvalene (**1a**) possesses an enthalpic barrier to degenerate Cope rearrangement (eq 28) of only 4.8-5.2 kcal mol.[60,61] This low barrier makes semibullvalene an obvious template for selective derivatization, such that a C_{2v} form (**2**) becomes the energy minimum. Since at such a C_{2v} geometry six electrons are cyclically delocalized, **2** is often described as being bishomoaromatic.[62,63]

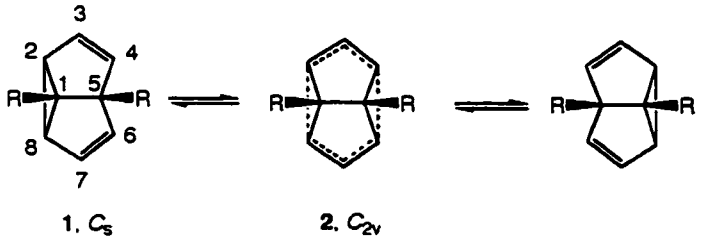

1. C_s 2. C_{2v}

(**a**) R = H (**b**) R = F (**c**) -RR- = -CH_2- (**d**) -RR- = -O-

eq 28

Based on qualitative molecular orbital theory arguments[64] and a variety of semiempirical calculations,[65,66,67,68] several substitution patterns have been proposed that should lower the energy of the C_{2v} geometry (**2**) relative to that of the C_s form (**1**). Hoffmann and Stohrer suggested that placing π radical stabilizing groups at the C_2, C_4, C_6, and C_8 positions of **1** should selectively stabilize **2**.[64] Indeed, it has been found experimentally that substitution of the C_2, C_4, C_6, and C_8 positions of **1** with groups such as phenyl[69] and cyano[70] lowers the barrier to Cope rearrangement to nearly zero.

Recently, density functional theory calculations have predicted that 2,6-dicyano-4,8-diphenyl-semibullvalene should, in fact, have a C_{2v} equilibrium geometry.[71]

Another result of the qualitative molecular orbital theory analysis of Hoffmann and Stohrer is that placement of σ electron withdrawing groups at the C_1 and C_5 positions should destabilize the cyclopropane ring in **1**. In fact, Hoffmann and Stohrer's Extended Hückel (EH)MO calculations indicated that placement of fluorines at the C_1 and C_5 positions of **1b** should result in **2b** being the equilibrium geometry.[64] Although AM1 calculations by Dewar and Jie found that **2b** lies 6 kcal/mol *higher* in energy than **1b**,[66] MP4 calculations by Szabo and Cremer predict that **2b** actually is the equilibrium geometry.[72]

Another strategy for making **2** the equilibrium geometry of a substituted semibullvalene is to destabilize the cyclopropane ring in **1** by adding short chains of one or two atoms.[67,68,73-75] For example, annelation of the C_1,C_5 positions of **1** with $-CH_2-$ affords 1,5-methanosemibullvalene (**1c**), which contains a [2.2]spiropentane moiety. The semiempirical calculations of Dannenberg *et al.*[67] predict that the resulting strain destabilizes **1c** sufficiently to make **2c** the equilibrium geometry.[67] Schleyer, Borden, and coworkers have reported the results of *ab initio* and density functional theory calculations on **2c** that support this semiempirical finding.[74]

Combining the strategies of destabilizing **1** by placing σ electron-withdrawing substituents at C_1 and C_5 and by adding a one-atom bridge across these two carbons suggests that the epoxide **1d** should display an even greater preference for a C_{2v} equilibrium geometry (**2d**) than either **1b** or **1c**. In this chapter, I report the results of *ab initio* and DFT calculations that were performed in order to test this conjecture.

I also carried out calculations aimed at assessing the degree of bishomoaromatic character of **2a-d**. Specifically, I computed the energies of isodesmic reactions that allow us to separate the effects of strain on destabilization of the C_s geometries of **1a-d** from the effects of bishomoaromaticity on stabilization of the C_{2v} geometries of **2a-d**. The results of my calculations, which are described in this chapter, predict that **1d** does have a much larger preference than **1a-c** for a C_{2v} equilibrium geometry; but my calculations find that **2c** and **2d** are both much less stabilized by bishomoaromaticity than either **2a** and **2b**.

Computational Methodology

All calculations were performed with the 6-31+G(d) basis set.[15,45] Calculations based on density functional theory were carried out with the three-parameter functional of Becke and the correlation functional of Lee, Yang, and Parr (B3LYP).[16] Geometries were optimized at the unrestricted (U)B3LYP level of theory by the standard methods implemented in the *Gaussian 98* suite of programs.[46] For all but **2c** and **2d**, the UB3LYP wave function converged to a restricted (R)B3LYP wave function with $\langle S^2 \rangle = 0.00$.

(U)B3LYP vibrational analyses were performed at each stationary point, in order to confirm its identity as a minimum or a transition state. The vibrational frequencies were used, without scaling, in order to convert energy differences into enthalpy differences at 298 K.

CASSCF and CASPT2[76] calculations were performed with the *MOLCAS* 5.0 suite of programs.[78] In the (6,6)CASSCF and (6,6)CASPT2 calculations on **1**, the six active electrons were distributed among the π and π^* orbitals of the two double bonds

and the σ and σ* orbitals of the unique cyclopropane ring bond. For the (6/6)CASSCF and (6/6)CASPT2 calculations on **2**, the orbitals in the active space were the three filled and three empty benzene-like MOs, formed from the orbitals of the two allylic π systems. For the (4/4) CASSCF and (4/4)CASPT2 calculations on bicyclo[3.3.0]octa-2,6-diene, the active space was comprised of four electrons, distributed among the π and π* orbitals of the two double bonds.

Since analytical gradients of CASPT2 energies with respect to nuclear displacements are not yet available, full CASPT2 geometry optimizations are impractical for molecules of the size of **1** and **2**. As was done previously,[74] partial CASPT2 geometry optimizations were performed on the lowest singlet state of **2** by fixing the C_2-C_8 and C_4-C_6 bond distances (*d*) at different values and using UB3LYP calculations to optimize the geometry of the remainder of the molecule at each value of *d*. (6/6)CASPT2 calculations were then performed at each of the partially optimized geometries, in order to determine which value of *d* gave the lowest (6/6)CASPT2 energy.

Geometries for the triplet states of **2** were optimized with UB3LYP calculations. Single-point (6/6)CASPT2 calculations were carried out at the UB3LYP optimized triplet geometries.

CASPT2 calculations on **1a-c** were performed at geometries optimized with restricted (R)B3LYP calculations. However, RB3LYP geometry optimizations did not locate a C_s minimum corresponding to **1d**; only a C_{2v} geometry (**2d**) was found. Nevertheless, it was possible to optimize a C_s geometry for **1d** by performing RHF calculations, since RHF calculations do not include the electron correlation that is necessary to describe the wave function for **2d** properly. Single-point (U)B3LYP and (6/6)CASPT2 calculations were then carried out at the optimized RHF geometry of **1d**.

In order to obtain a partially optimized (6,6)CASPT2 C_{2v} geometry for **2d**, geometry optimizations at different values of d were carried out with both UB3LYP and RHF calculations. Thus, two (6,6)CASPT2 geometries were obtained for **2d**, one that had been partially optimized with UB3LYP calculations and the other with RHF calculations. The former was found to have the lower (6,6)CASPT2 energy.

Results and Discussion

Energy Differences Between 2 and 1.

For each substituent, the B3LYP and CASPT2 energy differences between delocalized C_{2v} structure **2** and localized C_s semibullvalene **1** are given in Table 1. The optimized C_2-C_8 and C_4-C_6 bond distances (d) in **2** are also listed in Table 1. The geometries of **1a 2a** and **1c 2c** have previously been optimized at the B3LYP and CASPT2 levels of theory with the 6-31G(d) basis set by Schleyer, Borden, and co-workers.[74] Although I chose to augment this basis set with diffuse functions, my optimized B3LYP and CASPT2 geometries for these molecules are very close to those that have previously been published.

As shown in Table 1, unlike the case for the parent hydrocarbon, the C_{2v} geometry for 1,5-difluorosemibullvalene (**2b**) is predicted by both B3LYP and CASPT2 to be *ca.* 1 kcal mol lower in energy than the C_s geometry (**1b**). However, the possible errors in these calculations are at least this large, so that the prediction of a C_{2v} equilibrium geometry for **1b** should be regarded as equivocal. Nevertheless, the B3LYP and CASPT2 finding, that **2b** is lower in energy than **1b**, is consistent with the MP4 results of Szabo and Cremer.[72]

At both the B3LYP and CASPT2 levels the optimized interallylic distance (*d*) in **2b** is *ca.* 0.1 Å longer than *d* in **2a**. As noted previously,[4] the fact that the CASPT2 optimized value of *d* is slightly larger than the RB3LYP value probably reflects the greater ability of CASPT2 to represent a wave function that has diradical character.

The results of my UB3LYP calculations on **1c** and **2c** are in qualitative agreement with the previously reported RB3LYP results of Schleyer, Borden, and co-workers — the energy of the C_{2v} geometry is lower in energy than that of the C_s form.[4] However, my calculations find the energy of the UB3LYP optimized geometry of **2c** to be 3.6 kcal/mol lower than that of the geometry optimized with RB3LYP. In addition, the UB3LYP value of $d = 2.654$ in **2c** is 0.356 Å longer than the RB3LYP value of d=2.298 Å.

In contrast to the value of $\langle S^2 \rangle = 0.00$ found for the UB3LYP wave function at the optimized geometries of both **2a** and **2b**, $\langle S^2 \rangle = 1.03$ at the optimized geometry of **2c**. Thus, the "singlet" wave function for **2c** is an approximately 1:1 mixture of pure singlet ($\langle S^2 \rangle = 0$) and triplet ($\langle S^2 \rangle = 2$) states. The large amount of spin contamination in this wave function suggests that, in agreement with previous calculations,[15] **2c** has a large amount of diradical character.

At the CASPT2 level of theory, my calculations with the 6-31+G(d) basis set essentially reproduce the energy difference between **2c** and **1c** found by Schleyer *et al.* with the 6-31G(d) basis set. The 0.2 Å smaller interallylic distance, *d*, at the CASPT2 than at the UB3LYP level indicates that UB3LYP underestimates the interallylic bonding in **2c**. This is not surprising, since the UB3LYP wave function has 50% triplet character, whereas CASPT2 gives a pure singlet wave function.

As predicted, annelation of the C_1 and C_5 positions with O, rather than CH_2, is calculated to further lower the energy of **2** relative to **1**. I find that ΔE (**2d** - **1d**) = -20.3 and –22.1 kcal/mol at the UB3LYP and CASPT2 levels of theory, respectively.

Like the UB3LYP wave function for **2c**, the UB3LYP wave function for **2d** contains a great deal of triplet character. However, despite the slightly longer UB3LYP interallylic bond distance (d) in **2d** than in **2c**, $\langle S^2 \rangle$ = 0.87 for **2d** is smaller than $\langle S^2 \rangle$ = 1.03 for **2c**. Apparently, d is not the only factor that determines the amount of triplet character in the "singlet" UB3LYP wave function for **2** (*vide infra*).

Bonding Between the Allylic Fragments in 2 as Assessed by ΔE_{ST}

Table 1 shows that as the energy of the C_{2v} geometry (**2**) is lowered relative to the C_s geometry (**1**), the interallylic distances (d) in **2** increase. This finding suggests that interallylic bonding decreases on moving from **2a** to **2d**.

One way to assess the amount of interallylic bonding in **2** is to compute the adiabatic singlet-triplet energy difference, ΔE_{ST}. As the interallylic distance increases, one would expect that the two allyl fragments would interact less. Since there should be little or no interallylic interaction at the optimized geometry of the triplet state, ΔE_{ST} would be expected to decrease with increasing values of d in the singlet state.

For **2c** and **2d**, the large $\langle S^2 \rangle$ values for the UB3LYP "singlets" make the absolute UB3LYP values for ΔE_{ST} highly suspect. Nevertheless, as shown in Table 1, the UB3LYP values of ΔE_{ST} do show the same trend as the much more reliable CASPT2 values — **2b** > **2a** >> **2d** > **2c**. In fact, unlike the case in **2a**, **b**, and **d**, the ground state of

2c is predicted to be a triplet by both UB3LYP and CASPT2 calculations. The possibility of a triplet ground state for **2c** was not considered previously.[74-79]

It is surprising to find that the ground state of **2c** is predicted to be a triplet when, despite the larger interallylic distance in **2d** than in **2c**, the ground state of **2d** is predicted to be a singlet. However, this finding parallels the same type of inversion, already noted, in the amount of triplet character in the "singlet" UB3LYP wave functions for **2c** and **2d**.

Both ΔE_{ST} and $\langle S^2 \rangle$ in **2** are expected to depend on the difference in orbital energies between the HOMO and LUMO. Therefore, it is reasonable to seek the origin of the seemingly anomalous results for **2c** and **2d** by examining the changes that occur in the energies of these frontier orbitals upon substitution of $-CH_2-$ by $-O-$. Since the amount of interallylic bonding through space is apparently small at the large d values in both of these C_{2v} semibullvalenes, one must consider whether the difference between the through-bond interallylic interactions in the HOMO and/or the LUMO of **2c** and **2d** could be larger than the difference between the interallylic interactions through space.

As shown in Figure 1, the orbitals of the three-membered ring all lie in a nodal plane of the a_2 LUMO of the bisallylic fragment. Consequently, the ring orbitals do not affect the energy of this orbital in **2c** or **2d**. In contrast, the b_1 combinations of bonding and antibonding orbitals of the three-membered rings in **2c** and **2d** have the same symmetry as the HOMO of the bisallylic fragment. Interaction with the b_1 bonding orbital of the three-membered ring raises the energy of the bisallyl HOMO, whereas interaction with the b_1 antibonding ring orbital lowers the energy of the bisallyl HOMO.

In **2c** the interaction of the HOMO of the bisallylic fragment with the high-lying, b_1, bonding orbital of the cyclopropane ring orbitals is strong enough to raise the energy of the HOMO, relative to that of the LUMO, so that these orbitals are very close in

energy in **2c**. This is shown schematically on the left side of Figure 1. The energy difference between the HOMO and LUMO of **2c** (ΔE_{HL} = 23.3 kcal/mol) is apparently small enough that, as depicted in Figure 1, the ground state of **2c** is, in fact, predicted to be a triplet, by both UB3LYP and CASPT2 (Table 1).

Substitution of the oxygen atom in **2d** for the $-CH_2-$ group in **2c** affects the interactions between the HOMO of the bisallylic fragment and the b_1 ring orbitals in two ways. First, the electronegative oxygen lowers the energy of both the bonding and antibonding b_1 orbitals of the three-membered ring in **2d**, relative to the energies of these b_1 orbitals in **2c**. Second, the oxygen polarizes the bonding b_1 ring MO toward oxygen and away from C_1 and C_5, whereas the oxygen has the opposite effect on the antibonding b_1 ring MO.

The effects of the electronegativity of oxygen on the energies of the b_1 bonding and antibonding orbitals of the three-membered ring and on the contribution of C_1 and C_5 to these orbitals serve to decrease the interaction of the b_1 bonding orbital with the bisallyl HOMO and to increase the interaction of the b_1 antibonding orbital with the bisallyl HOMO.[80] Consequently, as shown schematically in Figure 1, substitution of –O– in **2d** for $-CH_2-$ in **2c** serves to lower the energy of the HOMO, relative to the LUMO.[81]

Thus, despite the effect of the large value of d on the strength of the interallylic bonding through space in **2d**, through-bond interactions serve to make the HOMO-LUMO gap large enough that a singlet ground state is predicted for **2d**. This prediction contrasts with that of a triplet ground state for **2c**, where through-bond interactions result in a smaller HOMO-LUMO gap.

The through-bond interactions in **2b**, involving the low-lying C-F σ^* orbitals,[82] are qualitatively similar to those in **2d**. Thus, despite the stronger interallylic interactions

through space in **2a**, through-bond interactions in **2b** make the HOMO-LUMO energy difference in **2b** much larger than in **2a.** This explains why **2b** has a 6 – 7 kcal/mol larger value of ΔE_{ST} than **2a**, even though d is ca. 0.1 Å longer in **2b** than in **2a**.

Assessment of the Bishomoaromatic Stabilization Energies (BHASEs) in 2 by Hydrogenation.

Another way to assess the strengths of the interallyic interactions in **2a-d** is to compute the hydrogenation energy of each of these C_{2v} species, relative to the hydrogenation energy of two isolated allyl radicals in appropriate reference compounds. I chose **5a-d**. The relative hydrogenation energies are given by the isodesmic reaction in eq 29, and the energies computed for this reaction are shown in Table 2.

eq 29

2 **3** **4** **5**

(**a**) R = H (**b**) R = F (**c**) -RR- = -CH_2- (**d**) -RR- = -O-

These energies represent the sum of the bonding interactions (both through space and through bonds) between the two allyl fragments in **2a - d**, minus any strain that is required to achieve these interactions. Although the net interallylic interaction energies, defined by eq 29, include through-bond contributions, I refer to them as the bishomoaromatic stabilization energies (BHASEs) of **2a - d**. I deem the CASPT2 values

to be more reliable than the (U)B3LYP values;[83] so, again, I base my discussion on the former.

Interestingly, the CASPT2 value of 15.4 kcal/mol for the BHASE in **2a** is almost the same as the interallylic interaction enthalpy in the boat Cope transition structure. Evaluated from experiments, the difference between the heats of formation of two allyl radicals[84] and the boat Cope transition structure[85] is 14.9 ± 2.1 kcal/mol, which is slightly larger than the (6/6)CASPT2/6-31G* value of 13.5 kcal/mol for the interallylic interaction enthalpy in the boat Cope transition structure.[86] Since the boat Cope rearrangement has $\Delta H^{\ddagger}$= 44.7 ± 2.0 kcal/mol,[85] the 40 kcal/mol lower enthalpy of activation for the degenerate rearrangement of semibullvalene (**1a**)[60,61] must be the result of a strain energy in **1a** of this size (*vide infra*).

Despite the 0.12 Å longer interallylic bond distance, d, in **2b** than in **2a**, the CASPT2 BHASE is computed to be 3.9 kcal/mol larger for **2b** than for **2a**. Apparently, electron donation from the bisallyl HOMO into the low-lying b_1 combination of C-F σ^* orbitals provides significantly more stabilization energy for **2b** than the interaction between the allyl SOMO and these σ^* orbitals furnishes for two molecules of **5b**. Presumably, it is this extra through-bond stabilization in **2b** that makes its BHASE greater than that of **2a**.[87]

In **2c** the BHASE is actually computed to be negative. This is also due to the effect of through-bond interactions, in this case involving the cyclopropane ring in **2c**. As shown in Figure 1, the filled b_1 orbital of the ring interacts with the bisallylic HOMO; and, since both orbitals are doubly occupied in the singlet state, this interaction provides no net stabilization for **2c**. In contrast, in **5c** the allyl nonbonding MO is only singly occupied; so the analogous interaction does provide some stabilization. Presumably, it is

this extra stabilization for the two molecules of **5c** in eq 29 that makes the isodesmic reaction in this equation slightly exothermic for **2c**.

The through-bond interactions, depicted schematically in Figure 1, involving the C-O σ* orbitals of the epoxide ring in **2d**, should stabilize **2d**, relative to **2c**. This selective stabilization of **2d** is probably the reason that its CASPT2 BHASE is 4.6 kcal mol larger than that of **2c**, despite the fact the CASPT2 interallylic bond distance in **2d** is ca. 0.1 Å larger than in **2c**.

Assessment of the Strain Energies (SEs) in 1.

Not only the BHASEs in the C_{2v} semibullvalenes (**2**), but also the SEs of the C_s semibullvalenes (**1**) contribute to the relative energies of **1** and **2**. The SEs of **1a-d** can be evaluated by computing the energies necessary to break the unique cyclopropane ring bonds in each semibullvalene, to form the hypothetical diradicals **6a-d**, in which the two allylic radicals do not interact with each other. The energy difference between **6** and **1** can then be compared with the energy necessary to break an unstrained C-C bond in an appropriate reference compound. I chose the central C-C bond in 1,5-hexadiene (**7**), cleavage of which forms two allyl radicals (**8**). Thus the SEs of **1a-d** are each defined as the energy of the isodesmic reaction in eq 30.

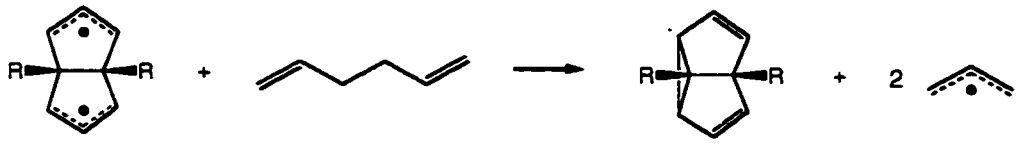

eq 30

6 **7** **1** **8**

(a) R = H **(b)** R = F **(c)** -RR- = -CH_2- **(d)** -RR- = -O-

The energies of **6a-d** can be estimated from the energies of **2a-d**, either by adding the relevant ΔE_{ST} value from Table 1, or by adding the appropriate BHASE value from Table 2. Except for **2b**, the two sets of numbers are nearly the same,[87] but I prefer to use the thermodynamic BHASE values in Table 2. If the strain energy of **1** is defined by

$$\begin{aligned} SE(\mathbf{1}) &= E(\mathbf{1}) - E(\mathbf{6}) + 2E(\mathbf{8}) - E(\mathbf{7}) \\ &= E(\mathbf{1}) - E(\mathbf{2}) - BHASE(\mathbf{2}) + 2E(\mathbf{8}) - E(\mathbf{7}) \end{aligned} \qquad \text{eq 31}$$

then adding BHASE(**2**) to SE(**1**) gives the net amount by which bishomoaromaticity and strain combine to make the energy difference between **1** and **2** smaller than that between 1,5-hexadiene (**7**) and two allyl radicals (**8**).

The (U)B3LYP/6-31 + G(d) bond dissociation energy of 1,5-hexadiene to two allyl radicals is computed to be 54.8 kcal/mol, and the corresponding enthalpy change for this reaction is calculated to be 49.6 kcal/mol. The use of a UB3LYP wave function for the radicals understimates the energy of this reaction. The (6/6)CASPT2/6-31+G(d) value of 58.0 kcal/mol for the bond dissociation energy is higher than the (U)B3LYP value but lower than the previously published (6/6)CASPT2/6-31G* value of 61.6 kcal/mol. The latter CASPT2 energy gives a value for the bond dissociation enthalpy in 1,5-hexadiene that is in better agreement with experiment than the former.[88] Therefore, I have chosen to use 2E(**8**) - E(**7**) = 61.6 kcal/mol in computing the CASPT2 SEs in Table 2.

Using the above UB3LYP and CASPT2 values for 2 E(**8**) - E(**7**), together with the values of E(**1**) - E(**2**) in Table 1 and the BHASE values for **2** in Table 2, the SEs for **1** in

Table 2 are obtained. For each type of calculation, 2E(**8**) - E(**7**) is an additive constant to all of the strain energies. Thus, eq 31 confirms that the difference between the SEs for any two semibullvalenes, plus the difference between their BHASEs, is equal to the difference between the relative energies of the C_s (**1**) and C_{2v} (**2**) geometries of the two semibullvalenes.

Whether the B3LYP energies or enthalpies or the CASPT2 energies are used, the data in Table 2 show that for each semibullvalene relief of strain in **1**, rather than bishomoaromatic stabilization in **2**, is the major reason why the energy difference between **2** and **1** is much smaller than the energy difference between 1,5-hexadiene (**7**) and two allyl radicals (**8**). However, for a more detailed discussion of the results in Table 2 I again use the presumably more accurate CASPT2 values for the BHASEs and SEs.

As noted in the previous section, since the CASPT2 BHASE in **2a** and the experimental allyl radical interaction enthalpy in the boat Cope transition structure are nearly the same, the difference of some 40 kcal/mol between the experimental activation enthalpies for the boat Cope[85] and semibullvalene[60,61] degenerate rearrangements must be due to roughly 40 kcal/mol of strain relief in going from **1a** to **2a**. This is, probably fortuitously, exactly the SE for **1a** found by my CASPT2 calculations.[89]

The (U)B3LYP calculations find the SEs of **1a** and **1b** to be almost identical. Thus, these calculations ascribe the negative activation enthalpy for the Cope rearrangement of **1b** entirely to a larger BHASE in **2b** than in **2a**. However, the CASPT2 results indicate that, on going from R = H to R = F, 3.1 kcal/mol of the 7.0 kcal/mol lower energy of **2**, relative to **1**, is due to greater relief of strain in **1b** than in **1a**. Since fluorine substituents are known to increase the strain in cyclopropane rings,[90] the CASPT2 finding seems more reasonable.

Through-bond interactions between the bisallylic HOMO and the bonds of the cyclopropane ring actually destabilize the lowest singlet state of **2c**, making the CASPT2 BHASE 21.0 kcal/mol smaller in **2c** than in **2b**. However, the 25.7 kcal/mol increase in strain on going from R = F to R-R = CH_2 makes the CASPT2 energy difference between **2c** and **1c** 4.7 kcal/mol larger than that between **2b** and **1b**.

Replacement of R-R = CH_2 in **2c** by R-R = O in **2d** results in through-bond interactions that stabilize the latter (see Figure 1). However, the resulting difference between the BHASEs of **2c** and **2d** accounts for only 4.6 kcal/mol of the 16.5 kcal/mol difference between the relative energies of **1c-2c** and **1d-2d**. The balance of 11.9 kcal/mol is due to the increase in strain that occurs when R-R = CH_2 in **1c** is replaced by R-R = O in **1d**.

Conclusions

Our calculations find that 1,5-annelated semibullvalenes **1c** and **1d** each have a large energetic preference for a C_{2v} equilibrium geometry, respectively **2c** and **2d**. However, **2c** and **2d** both have significantly reduced BHASEs, relative to the C_{2v} transition state (**2a**) for the degenerate Cope rearrangement of the parent semibullvalene (**1a**).[91] The driving force for conversion of **1c** to **2c** and **1d** to **2d** is not bishomoaromatic stabilization of the C_{2v} geometries, but rather relief of strain in the C_s geometries of the semibullvalenes. Therefore, the common practice of describing all semibullvalenes that prefer a C_{2v} geometry as "bishomoaromatic" is misleading.

In fact, interallylic bonding through space is so small in **2c** that through-bond interactions are predicted to make the ground state of this diradical a triplet. I hope that this prediction will be tested experimentally.

On the other hand, my CASPT2 calculations find that through-bond interactions in **2b**, involving the fluorines, make the BHASE in this semibullvalene greater than that in **2a.** The increased BHASE in **2b**, coupled with an increased SE in **1b**, relative to **1a**, are predicted to make the C_{2v} structure the equilibrium geometry, albeit by only 1-2 kcal mol. Like the prediction of a triplet ground state for **2c**, I hope the prediction that semibullvalene **1b** will prefer a geometry (**2b**) which not only has C_{2v} symmetry but is also bishomoaromatic, will be subject to experimental test.

Table 6. Energy and Enthalpy Differences Between C_s (**1**) and C_{2v} (**2**) Semibullvalenes, and C_2-C_8 (= C_4-C_6) Bond Distances (d), $\langle S^2 \rangle$, and Adiabatic Singlet-Triplet Energy Differences (ΔE_{ST}) in **2**. (6,6)CASPT2/6-31+G(d) Values are Given in Italics Below the UB3LYP/6-31+G(d) Values.

Substituents at C_1 and C_5	ΔE(**2**-**1**) (kcal mol)	ΔH^{298}(**2**-**1**) (kcal mol)	d (Å)	$\langle S^2 \rangle$ (a. u.)	ΔE_{ST} (kcal mol)
R = H	5.0	3.9[a]	2.117	0.00	12.3
	6.1		*2.122*	–	*15.7*
R = F	-0.8	-1.7	2.216	0.00	19.3
	-0.9		*2.243*	–	*21.4*
RR = $-CH_2-$	-5.9	-7.4	2.654	1.03	-1.5
	-5.6		*2.472*	–	*-1.3*
RR = –O–	-20.3	-19.5[b]	2.661	0.87	1.8
	-22.1[c]		*2.574*	–	*3.3*
	-19.9[d]		*2.585*		

[a] $\Delta H^{\ddagger}$.

[b] Based on scaling the RHF vibrational frequencies for **1d** by 0.8929

[c] CASPT2: RHF energy for **1d** and CASPT2: CASPT2-UB3LYP energy for **2d**.

[d] CASPT2: RHF energy for **1d** and CASPT2: CASPT2-RHF energy for **2d**.

Table 7. Bishomoaromatic Stabilization Energies and Enthalpies (BHASEs) for the C_{2v} Semibullvalenes (**2**)[a] and Strain Energies and Enthalpies (SEs)[b] for the C_s Semibullvalenes (**1**). CASPT2 Values are Given in Italics Below the UB3LYP Values.

	BHASEs		SEs	
R	ΔE	ΔH^{298}	ΔE	ΔH^{298}
H	10.9	10.0	38.9	35.7
	15.4		*40.1*	
F	16.9	15.5	38.7	35.8
	19.3		*43.2*	
RR = $-CH_2-$	-2.0	-1.8	62.7	58.8
	-1.7		*68.9*	
RR = $-O-$	1.3	1.2	73.8	67.9[c]
	2.9		*80.8*	

[a]Computed from the energy enthalpy of the isodesmic reaction in eq 29.

[b]Computed from the energy enthalpy of the isodesmic reaction in eq 30.

[c]Based on scaling the RHF vibrational frequencies in **1d** by 0.8929.

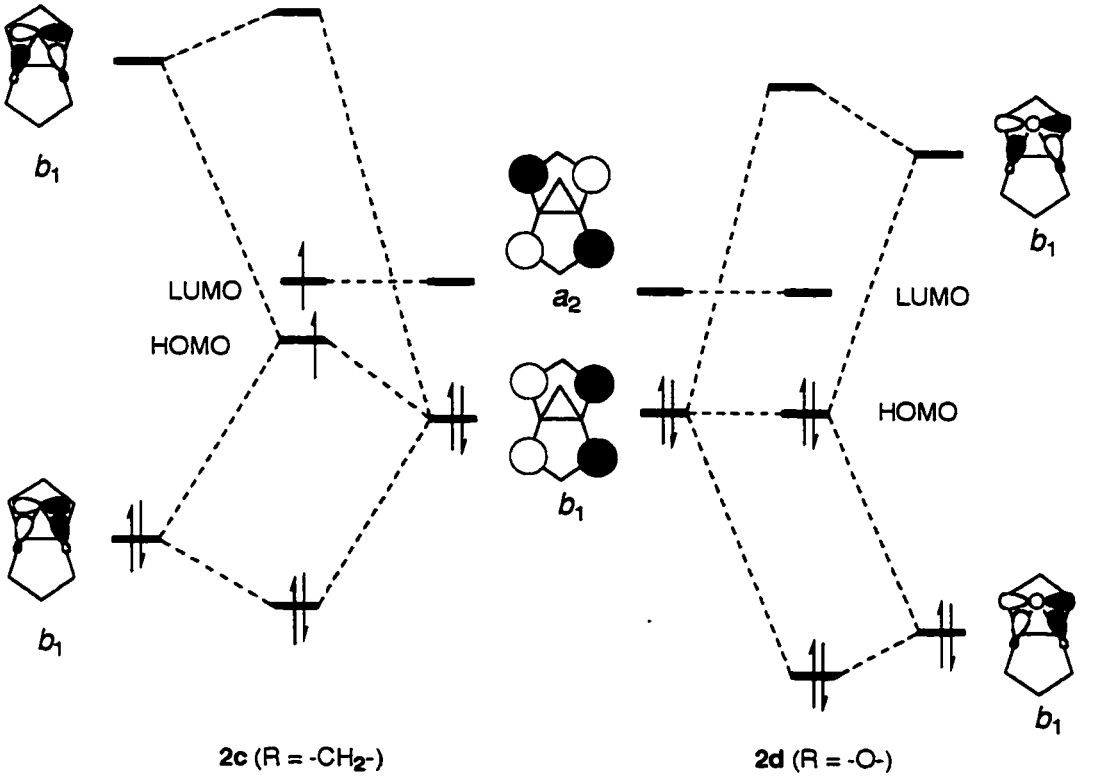

Figure 4. Schematic Representation of the Interactions of the Out-of-Phase Combinations of the σ and σ^* orbitals between the bridgehead carbons and the bridging group (CH_2 in **2c** and O in **2d**) with the HOMO and LUMO, formed by through-space interactions between the π orbitals of the two allyl groups.

V. Summary

The research reported in this dissertation is concerned with molecules in which heteroatom substitution results in a substituted system that has very different properties from the original molecule. For example, replacement of a carbon in benzene by silicon results in a very unstable hydrocarbon becoming an organosilane that can only be studied in matrix isolation, unless it is kinetically stabilized by steric blockade. Moreover, substitutuion of phosphorus for silicon results in phosphabenzene, a molecule who kinetic stability is only slightly less than that of benzene.

Electronic structure calculations, the results of which are described in Chapter II, rationalize the differences in reactivity, caused by heteroatom substitution, and quantitatively analyze the different contributors to them. *Providing explanations for puzzling observations is an important application of any theoretical method.*

Another function of theory is to make predictions that are experimentally testable and that are likely to stimulate experiments. Examples of this type of application of electronic structure calculations are provided in Chapters III and IV.

Chapter III predicts how heteroatom substitution should alter the doublet-quartet splitting in heteroatom analogues of TMM radical cation and radical anion. The calculations further predict that the quartet can, at least in principle, become the ground state of suitable substituted derivatives of TMM radical anion, but no derivative of TMM radical cation will be found to have a quartet ground state.

The calculations described in Chapter IV make predictions as to how the substitution of fluorine for hydrogen at C_1 and C_5 of semibullvalene and the substitution of oxygen for CH_2 in methanosemibullvalene will affect the equilibrium geometries and electronic structures. In both cases calculations find heteroatoms substitution has two effects–it increases the strain at the C_s geometry of the localized semibullvalene, and it results in stabilization of the bisallyl HOMO via through-bond interactions.

Both effects are predicted to stabilize the C_{2v} geometry of the delocalized semibullvalene, relative to the C_s geometry of the localized semibullvalene; and the through-bond interactions are predicted to stabilize the lowest singlet state at this delocalized geometry. In methanosemibullvalene the effect of substituting oxygen for CH_2 is predicted to be particularly dramatic, since the hydrocarbon is calculated to have a triplet ground state; but, a singlet ground state is computed for the oxa-heteroatom analogue.

The predictions made in Chapters III and IV are experimentally testable, and it is to be hoped that they will lead to experiments designed to test them.

End Notes

(1) μ=0.735 ± 0.01 Debye. Weast, R. C., Ed. *Handbook of Chemistry and Physics, 66th Edition*: CRC Press: Boca Raton, **1985**, E-59.

(2) A notable exception to this simple picture is carbon monoxide (CO). While it is true that the electronegativity of oxygen is greater than that of carbon, it turns out that the resonance contributor depicted by $C{\equiv}O^{+}$ is sufficiently prevalent to effect a dipole moment with its magnitude in the direction of the carbon atom.

(3)This can be thought of as the product of a nuclear fusion reaction where the proton of the H atom in CH has been transferred into the carbon nucleus while the electron pair in the C-H bond remains in place.

(4) See: Helgaker, T.; Jørgensen, P. Olsen, J. *Molecular Electronic-Structure Theory*: John Wiley and Sons, Ltd.: Chichester, **2000**.

(5) For a lucid exposition, see: Koch, W.; Holthausen, M. C. *A Chemist's Guide to Density Functional Theory, Second Edition*: Wiley-VCH: Weinheim, **2001**.

(6) Review: Raabe, G.; Michl, J. *Chem. Rev.* **1985**, *85*, 419.

(7) (a) Cowley, A. H. *Polyhedron* **1984**, *3*, 389. (b) Cowley, A. H. *Acc. Chem. Res.* **1984**, *17*, 386.

(8) (a) Sun, H.; Hrovat, D. A.; Borden, W. T. *J. Am. Chem. Soc.* **1987**, *109*, 5275. For related calculations at higher levels of theory, see: (b) Schmidt, M. W.; Truong, P. N.; Gordon, M. S. **1987**, *109*, 5217 and Wiberg, K. B.; Nakaji, D. *J. Am. Chem. Soc.* **1993**, *115*, 10658.

(9) (a) Maier, G.; Mihm, G.; Reisenauer, H. P. *Angew. Chem. Int. Ed Engl.* **1980**, *19*, 52. (b) Kreil, C. L.; Chapman, O. L.; Burns, G. T.; Barton, T. J. *J. Am. Chem. Soc.* **1980**, *102*, 841. (c) Maier, G.; Mihm, G.; Reisenauer, H. P. *Chem. Ber.* **1982**, *115*, 801. (d) Maier, G.; Mihm, G.; Baumgartener, R. O. W.; Reisenauer, H. P. *Chem. Ber.* **1984**, *117*, 2337.

(10) Märkl, G.; Schlosser, W. *Angew. Chem. Int. Ed Engl.* **1988**, *27*, 963.

(11) A silanaphthalene, substituted on silicon with the massively bulky 2,4,6-tris[bis(trimethylsilyl)methyl]phenyl group, has recently been found to be stable to dimerization, even upon heating. Tokitoh, N.; Wakita, K.; Okazaki, R.; Nagase, S.; Schleyer, P. von R.; Jiao, H. *J. Am. Chem. Soc.* **1997**, *119*, 6851.

(12) Review: Ashe, A. J., III, *Acc. Chem. Res.* **1978**, *11*, 153.

(13) (a) Ashe, A. J., III, Gordon, M. D. *J. Am. Chem. Soc.* **1972**, *94*, 7596. (b) The 2,4,6-triphenyl derivative also undergoes this reaction; Märkl, G.; Lieb, F. *Angew. Chem. Int. Ed Engl.* **1968**, *7*, 733.

(14) Frisch, M. J.; Trucks, G. W.; Schlegel, H. B.; Scuseria, G. E.; Robb, M. A.; Cheeseman, J. R.; Zakrzewski, V. G.; Montgomery, J. A., Jr.; Stratmann, R. E.; Burant, J. C.; Dapprich, S.; Millam, J. M.; Daniels, A. D.; Kudin, K. N.; Strain, M. C.; Farkas, O.; Tomasi, J.; Barone, V.; Cossi, M.; Cammi, R.; Mennucci, B.; Pomelli, C.; Adamo, C.; Clifford, S.; Ochterski, J.; Petersson, G. A.; Ayala, P. Y.; Cui, Q.; Morokuma, K.; Malick, D. K.; Rabuck, A. D.; Raghavachari, K.; Foresman, J. B.; Cioslowski, J.; Ortiz, J. V.; Stefanov, J. V.; Liu, G.; Liashenko, A.; Piskorz, P.; Komaromi, I.; Gomperts, R.; Martin, R. L.; Fox, D. J.; Keith, T.; Al-Laham, M. A.; Peng, C. Y.; Nanayakkara, A.;

Gonzalez, C.; Challacombe, M.; Gill, P. M. W.; Johnson, B.; Chen, W.; Wong, M. W.; Andres, J. L.; Gonzalez, C.; Head-Gordon, M.; Replogle, E. S.; Pople, J. A. *Gaussian 98, Revision A.6*; Gaussian, Inc.: Pittsburgh, PA, 1998.

(15) Harihan, P. C.; Pople, J. A. *Theor. Chim. Acta* **1973**, *28*, 213.

(16) (a) Becke, A. D. *J. Chem. Phys.* **1993**, *98*, 5648. (b) Lee, C.; Yang, W.; Parr, R. G. *Phys. Rev. B* **1988**, *37*, 785.

(17) The exothermicity calculated for the reaction in eq 4 is about ten times larger than the value of ΔH = -2.6 kcal mol computed for the analogous isodesmic reaction that gives the difference between the heats of hydrogen addition to the first-period congeners, pyridine and benzene.

(18) Benson, S. W. *Thermochemical Kinetics*, 2nd ed.; Wiley: New York, 1976.

(19) Römer, B.; Gatev, G. G.; Zhong, M.; Brauman, J. I. *J. Am. Chem. Soc.* **1998**, *120*, 2919.

(20) See, *inter alia*, (a) Cherry, W.; Epiotis, N. D.; Borden, W. T. *Acc. Chem. Res.* **1977**, *10*, 167. (b) Feller, D.; Davidson, E. R.; Borden, W. T. *J. Am. Chem. Soc.* **1985**, *107*, 2596. (c) Coolidge, M. B.; Borden, W. T. *J. Am. Chem. Soc.* **1990**, *112*, 1704. (d) Coolidge, M. B.; Hrovat, D. A.; Borden, W. T. *J. Am. Chem. Soc.* **1992**, *114*, 2354. (e) Johnson, W. T. G.; Borden, W. T. *J. Am. Chem. Soc.* **1997**, *119*, 5930. (f) Review: Borden, W. T. *Chem. Commun.* **1998**, 1919

(21) (a) Sakurai, H.; Murakami, M. *J. Am. Chem. Soc.* **1969**, *91*, 519. (b) Brook, A. G; Duff, J. H. *J. Am. Chem. Soc.* **1969**, *91*, 2119. (c) Krusic, P. G.; Kochi, J. K. *J. Am. Chem. Soc.* **1969**, *91*, 3938.

(22) For a glaring exception to this generalization and a discussion see Kemnitz, C. R.; Karney, W. L.; Borden, W. T. *J. Am. Chem. Soc.* **1998**, *120*, 3499.

(23) Kutzelnigg, W. *Angew. Chem. Int. Ed. Engl.* **1984**, *23*, 272.

(24) Berkowitz, J.; Ellison, G. B.; Gutman, D. *J. Phys. Chem.* **1994**, *98*, 2744.

(25) (a) Chase, M. W., Jr. *NIST-JANAF Themochemical Tables, Fourth Edition, J. Chem. Phys. Ref. Data, Monograph 9*, **1998**. The value given by Chase is actually DH^{298} (H_2P-H) = 76.7 kcal mol. DH^{298} (H_2P-H) = 80.9 kcal mol is obtained by using the value of $\Delta Hf^{298}(PH_3)$ = 1.3,[19] which is based on red phosphorus, rather than the value $\Delta Hf^{298}(PH_3)$ = 5.5 kcal mol, which is based on white phosphorus and was employed by Chase.

(26) Curtiss, L. A.; Raghavachari, K.; Trucks, G. W.; Pople, J. A. *J. Chem. Phys.* **1991**, *94*, 7221.

(27) (a) Coolidge, M. B.; Borden, W. T. *J. Am. Chem. Soc.* **1988**, *110*. 2298. (b) A previous DFT study of the effect of substituents on Si-H BDEs has also been published, Wu, Y.-D.; C.-H. Ling, *J. Org. Chem.* **1995**, *60*, 821.

(28) (a) Ding, L.; Marshall, P. *J. Am. Chem. Soc.* **1992**, *114*. 5754. (b) Goumri, A.; Yuan, W.-J.; Marshall, P. *J. Am. Chem. Soc.* **1993**, *115*, 2539.

(29) For earlier experimental studies of the effects of alkyl substituents on Si-H BDEs, see (a) Walsh, R. A. *Acc. Chem. Res.* **1981**, *14*, 246. (b) Wetzel, D. M.; Salomon, K. E.; Brauman, J. I. *J. Am. Chem. Soc.* **1989**, *111*, 3835.

(30) Bent, H. A. *Chem. Rev.* **1961**, *61*, 275.

(31) Berger, S.; Brauman, J. I. *J. Am. Chem. Soc.* **1992**, *114*, 4737.

(32) See, for example, (a) Nicolaides, A.; Borden, W. T. *J. Am. Chem. Soc.* **1991**, *113*, 6750. (b) Hrovat, D. A.; Duncan, J. A.; Borden, W. T. *J. Am. Chem. Soc.* **1999**, *121*, 169. (c) Ref 20e.

(33) See: Coulson, C. A. *J. Chim. Phys.* **1948**, *45*, 243.

(34) Dowd, P. *J. Am. Chem. Soc.* **1966**, *88*, 2587.

(35) For reviews, see for example: (a) Dowd, P. *Acc. Chem. Res.* **1972**, *5*, 242. (b) Berson, J. A. *Acc. Chem. Res.* **1978**, *11*, 446. (c) Borden, W. T.; Davidson, E. R. *Acc.*

Chem. Res. **1981**, *14*, 69. (d) Berson, J. A. In *Diradicals*; Borden, W. T., Ed.; J. Wiley and Sons: New York, **1982**; Chapter 4.

(36) (a) Dowd, P.; Sachdev, K. *J. Am. Chem. Soc.* **1967**, *89*, 715. (b) Dowd, P.; Gold, A.; Sachdev, K. *J. Am. Chem. Soc.* **1968**, *90*, 2715. (c) Basemen, R. J.; Pratt, D. W.; Chow, M.; Dowd, P. *J. Am. Chem. Soc.* **1976**, *98*, 5726.

(37) See, for example: (a) Davidson, E. R.; Borden, W. T.; *J. Am. Chem. Soc.* **1977**, *99*, 2053. (b) Borden, W. T. In *Diradicals*; Borden, W. T., Ed.; J. Wiley and Sons: New York, **1982**; pp. 1-72.

(38) Ovchinnikov, A. A. *Theoret. Chim. Acta* **1978**, *47*, 297.

(39) (a) Wenthold, P. G.; Hu, J.; Squires, R. R.; Lineberger, W. C. *J. Am. Chem. Soc.* **1996**, *118*, 475. (b) Wenthold, P. G.; Hu., J; Squires, R. R; Lineberger, W. C. *J. Am. Soc. Mass Spectrom.* **1999**, *10*, 800-809.

(40) (a) Cramer, C. J.; Smith, B. A. *J. Phys. Chem.* **1996**, *100*, 9664. (b) For a recent review of singlet-triplet splittings in non-Kekule hydrocarbon diradicals, see: Borden, W.

T. In *Magnetic Properties of Organic Materials*; Lahti, P., Ed..; Marcel Dekker, Inc.: New York, **1999**; pp. 61-102.

(41) Komaguchi, K.; Shiotani, M.; Lund, A. *Chem. Phys. Lett.* **1997**, *265*, 217.

(42) Du, P.; Borden, W. T. *J. Am. Chem. Soc.* **1987**, *109*, 5330.

(43) (a) Takahashi, Y.; Miyashi, T.; Mukai, T. *J. Am. Chem. Soc.* **1983**, *105*, 6511. (b) Miyashi, T.; Takahashi, Y.; Mukai, T.; Roth, H. D.; Schilling, M. L. M. *J. Am. Chem. Soc.* **1985**, *107*, 1079. (c) Miyashi, T.; Kamata, M.; Mukai, T. *J. Am. Chem. Soc.* **1986**, *108*, 2755.

(44) Itoh, T.; Matsuda, K.; Iwamura, H.; Hori, K. *J. Am. Chem. Soc.* **2000**, *122*, 2567.

(45) Clark, T.; Chandrasekhar, J.; Spitznagel, G. W.; Schleyer, P. v. R. *J. Comput. Chem.* **1983**, *4*, 294.

(46) Frisch, M. J.; Trucks, G. W.; Schlegel, H. B.; Scuseria, G. E.; Robb, M. A.; Cheeseman, J. R.; Zakrzewski, V. G.; Montgomery, J. A., Jr.; Stratmann, R. E.; Burant,

J. C.; Dapprich, S.; Millam, J. M.; Daniels, A. D.; Kudin, K. N.; Strain, M. C.; Farkas, O.; Tomasi, J.; Barone, V.; Cossi, M.; Cammi, R.; Mennucci, B.; Pomelli, C.; Adamo, C.; Clifford, S.; Ochterski, J.; Petersson, G. A.; Ayala, P. Y.; Cui, Q.; Morokuma, K.; Malick, D. K.; Rabuck, A. D.; Raghavachari, K.; Foresman, J. B.; Cioslowski, J.; Ortiz, J. V.; Stefanov, J. V.; Liu, G.; Liashenko, A.; Piskorz, P.; Komaromi, I.; Gomperts, R.; Martin, R. L.; Fox, D. J.; Keith, T.; Al-Laham, M. A.; Peng, C. Y.; Nanayakkara, A.; Gonzalez, C.; Challacombe, M.; Gill, P. M. W.; Johnson, B.; Chen, W.; Wong, M. W.; Andres, J. L.; Gonzalez, C.; Head-Gordon, M.; Replogle, E. S.; Pople, J. A. *Gaussian 98, Revision A.7*; Gaussian, Inc.: Pittsburgh, PA, 1998.

(47) (a) Schmidt, M. W.; Baldridge, K. K.; Boatz, J. A.; Elbert, S. T.; Gordon, M. S.; Jensen, J. H.; Koseki, S.; Matsunga, N.; Nguyen, K. A.; Su, S. J.; Windus, T. L.; Dupuis, M.; Montgomery, J. A. *J. Comput. Chem.* **1993**, *14*, 1347. (b) Bode, B. M.; Gordon, M. S. *J. Mol. Graphics Mod.* **1999**, *16*, 133.

(48) Borden, W. T.; Davidson, E. R. *Acc. Chem. Res.* **1996**, *29*, 67.

(49) (a) Andersson, K.; Malmqvist, P-Å.; Roos, B. O.; Sadlej, A. J.; Wolinski, K. *J. Phys. Chem.* **1990**, *94*, 5483. (b) Andersson, K.; Malmqvist, P.-Å.; Roos, B. O. *J. Chem. Phys.* **1992**, *96*, 1218.

(50) Andersson, K.; Blomberg, M. R. A.; Fülscher, M. P.; Karlström, G.; Lindh, R.; Malmqvist, P.-Å.; Neogrády, P.; Olsen, J.; Roos, B. O.; Sadlej, A. J.; Schütz, M.; Seijo, L.; Serrano-Andrés, L.; Siegbahn, P. E. M.; Widmark, P.-O. *MOLCAS*, version 4.1; Department of Theoretical Chemistry, Chemical Centre: University of Lund, P.O.B. 124, S-221 00 Lund, Sweden, 1997.

(51) For detailed discussions of artifactual symmetry breaking in similar molecules, see: Davidson, E. R.; Borden, W. T. *J. Phys. Chem.* **1983**, *87*, 4783.

(52) Jahn, H. A.; Teller, E. *Proc. R. Soc. London, Ser. A* **1937**, *116*, 605.

(53) See, for example: (a) Schmidt, M. W.; Truong, P. N.; Gordon, M. S. **1987**, *109*, 5217. (b) Wiberg, K. B.; Nakaji, D. *J. Am. Chem. Soc.* **1993**, *115*, 10658.

(54) This H_3 · model breaks down if distortions from D_{3h} geometries are allowed; since the Jahn-Teller-active vibrational modes in $^2E'$ lead to stationary points with highly distorted geometries. One stationary point corresponds to a hydrogen molecule plus a distant hydrogen atom at a C_{2v} geometry, and another stationary point corresponds to a linear geometry, with equal H-H bond lengths, that is the transition structure for the H_2 + H · reaction.

(55) It is easy to use eqs 2 and 3 to show that electrons of opposite spin can appear simultaneously in the overlap regions between ϕ_1 and ϕ_2 and between ϕ_1 and ϕ_3 in $^2\Psi_x$ and between ϕ_2 and ϕ_3 in $^2\Psi_y$.

(56) If overlap were included in normalizing the MOs in eqs 4 - 6, in eqs. 7 - 9 the coefficients of ψ_1 would increase, and those of ψ_2 and ψ_3 would decrease. Therefore, with inclusion of overlap in the normalization, the weight of the first configuration in eqs. 11 and 12 would be larger than the weight of the second configuration; and the combined weights of the last two configurations would have an intermediate value. Consequently, when overlap is significant, constraining the weights of the configurations in eqs 11 and 12 to be equal disadvantages these doublet wavefunctions, relative to the quartet, by making the doublets overall slightly antibonding, rather than nonbonding.

(57) Squires *et al.* have measured EA= 9.9 kcal/mol for $C(CH_2)_3^{\cdot -}$,[39] in fair agreement with the value of EA= 5.3 kcal/mol, computed by UB3LYP. The agreement between the calculated and experimental EAs is further improved if the CH_2 groups in $C(CH_2)_3^{\cdot -}$ are allowed to pyramidalize, which lowers the energy of the radical anion by 0.4 kcal/mol, and gives EA= 5.7 kcal/mol.

(58) Unconstrained reoptimization of the geometry of the quartet led to a C_1 structure, with all the silyl centers pyramidalized, which was 46.4 kcal/mol lower in energy than planar $^4A_2''$. Attempts to reoptimize the geometry of the lowest planar doublet led, unfortunately, to pyramidalization accompanied by Si-Si bond formation. However, constrained optimization of a $^2A''$ wavefunction, with a plane of symmetry perpendicular to the molecular plane, led to a C_s geometry with the two equivalent silyls pyramidalized in the opposite direction than the third. The energy of this doublet was computed to be 0.2 kcal/mol lower than that of the fully optimized quartet.

(59) In $O(SiH_2)^{\cdot +}$, the two unique bond lengths at the CASSCF-optimized C_{2v} geometry of the $^2A_2$ state (R = 1.788 Å and 1.789 Å) are computed to be only slightly longer than those in the same state of $AlO_3^{\cdot}$ (R = 1.741 Å and 1.742Å). When the CASSCF

calculation on $O(SiH_2)^{\bullet+}$ was repeated at the CASSCF-optimized geometry of $AlO_3^{\bullet}$, the ratio $(c_2\ c_1)^2$ at the equilibrium geometry of $O(SiH_2)^{\bullet+}$ was essentially unchanged.

(60) Cheng, A. K.; Anet, F. A. L.; Mioduski, J.; Meinwald, J. *J. Am. Chem.Soc.* **1974**, *96*, 2887.

(61) Moskau, D.; Aydin, R.; Leber, W.; Günther, H.; Quast, H.; Martin, H.-D.; Hassenrück, K.; Miller, L. S.; Grohmann, K. *Chem. Ber.* **1989**, *122*, 925.

(62) Reviews: (a) Williams, R. V. *Chem. Rev.* **2001**, *101*, 1185. (b) Williams, R. V. *Adv. Theor. Interesting Mol.* **1998**, *4*, 157. (c) Williams, R. V. *Eur. J. Org. Chem.* **2001**, 227. (d) Childs, R. F.; Cremer, D.; Elia, G. In *The Chemistry of the Cyclopropyl Group*; Rappoport, Z., Ed.; J. Wiley & Sons: Chichester, **1995**; Vol. 2, 411.

(63) Experimental evidence has recently been presented that benzene oxide provides an example of a neutral molecule with an equilibrium geometry that is homoaromatic: (a) More O'Ferrall, R. A.; Rao, S. N. *Croat. Chem. Acta* **1992**, *65*, 593. (b) Rao, S. N.; More O'Ferrall, R. A.; Kelly, S. C.; Boyd, D. R.; Agarwal, R. *J. Am. Chem. Soc.* **1993**, *115*, 5458. (c) Jia, Z. S.; Brandt, P.; Thibblin, A. *J. Am. Chem. Soc.* **2001**, *123*, 10147.

(64) Hoffmann, R.; Stohrer, W. D. *J. Am. Chem. Soc.* **1971**, *93*, 6941.

(65) Dewar, M. J. S.; Lo, D. H. *J. Am. Chem. Soc.* **1971**, *93*, 7201.

(66) Dewar, M. J. S.; Jie, C. *Tetrahedron* **1988**, *44*, 1351.

(67) Miller, L. S.; Grohmann, K.; Dannenberg, J. J. *J. Am. Chem. Soc.* **1983**, *105*, 6862.

(68) (a) Williams, R. V.; Kurtz, H. A. *J. Org. Chem.* **1988**, *52*, 3226. (b) Williams, R. V.; Kurtz, H. A. *J. Chem. Soc. Perkin Trans. 2* **1994**, 147.

(69) Quast, H.; Seefelder, M. *Angew. Chem. Int. Ed.* **1999**, *38*, 1064.

(70) Quast, H.; Janiak, R.; Peters, E.-M.; Peters, K.; von Schnering, H. G. *Chem. Ber.* **1992**, *125*, 969.

(71) (a) Hrovat, D. A.; Williams, R. V.; Goren, A. C.; Borden, W. T. *J. Comp. Chem.* **2001**, *22*, 1565. (b) Goren, A. C.; Hrovat, D. A.; Seefelder, M.; Quast, H.; Borden, W. T. *J. Am. Chem. Soc.* **2002**, *124*, 3469.

(72) Szabo, K. J.; Cremer, D., unpublished results cited in ref. 62d.

(73) Williams, R. V.; Gadgil, V. R.; Chauhan, K.; Jackman, L. M.; Fernandes, E. *J. Org. Chem.* **1998**, *63*, 3302.

(74) Jiao, H.; Nagelkerke, R.; Kurtz, H. A.; Williams, R. V.; Borden, W. T.; Schleyer, P. v. R. *J. Am. Chem. Soc.* **1997**, *119*, 5921.

(75) For very recent calculations on the effect of additional bridges on a degenerate divinylcyclobutane Cope rearrangement, see: Tantillo, D. J.; Hoffmann, R. *J. Org. Chem.* **2002**, *67*, 1419.

(76) (a) Andersson, K.; Malmqvist, P-Å.; Roos, B. O.; Sadlej, A. J.; Wolinski, K. *J. Phys. Chem.* **1990**, *94*, 5483. (b) Andersson, K.; Malmqvist, P.-Å.; Roos, B. O. *J. Chem. Phys.* **1992**, *96*, 1218.

(77) CASPT2 calculations include the effects of dynamic electron correlation. See ref. 48 and references cited therein.

(78) Andersson, K.; Blomberg, M. R. A.; Fülscher, M. P.; Karlström, G.; Lindh, R.; Malmqvist, P.-Å.; Neogrády, P.; Olsen, J.; Roos, B. O.; Sadlej, A. J.; Schütz, M.; Seijo, L.; Serrano-Andrés, L.; Siegbahn, P. E. M.; Widmark, P.-O. MOLCAS, version 5.0; Department of Theoretical Chemistry, Chemical Centre: University of Lund, P.O.B. 124, S-221 00 Lund, Sweden, **1997**.

(79) I have investigated the possibility that 2,6-dicyano-4,8-diphenylsemibullvalene^{-1} also possesses a low-lying triplet state. Indeed, ΔE_{ST} = 2.1 kcal/mol at the UB3LYP/6-31G* level, with $\langle S^2 \rangle$ = 0.67 for the "singlet." Clearly the intraallylic electron delocalization in this semibullvalene reduces the interallylic bonding interactions, relative to those in **2a**.

(80) The latter interaction provides net stabilization of **2d**, relative to **2c**. Similarly, replacement of the CH_2 group in norcaradiene by the oxygen atom in benzene oxide should selectively stabilize for the latter molecule by enhancing the interaction between the HOMO of butadiene and the LUMO of the three-membered ring. This interaction

probably provides at least some of the enthalpic stabilization that has been measured for benzene oxide.[93]

(81) The energy of the bisallyl HOMO is also lowered upon decreasing the interallyllic distance, d, in **2**; and the energy of the bisallyl LUMO is raised. Since d is different at the equilibrium geometries of **2a-d**, calculating the HOMO-LUMO energy difference (ΔE_{HL}) at the equilibrium geometry of each C_{2v} semibullvalene does not provide a straightforward assessment of how substitution of H in **2a** by F in **2b** and the CH_2 group in **2c** by O in **2d** affects the through-bond interactions in these semibullvalenes. The most straightforward way to compare the effect of through-bond interactions on the values of ΔE_{HL} in two different C_{2v} semibullvalenes is to perform calculations on both at the equilibrium geometry of just one of them. For example, using the Kohn-Sham orbital energies from B3LYP calculations on the triplet states, ΔE_{HL}(**2a**) = 75.3 kcal/mol and ΔE_{HL}(**2b**) = 85.7 kcal/mol at d = 2.122 Å, the CASPT2-optimized interallylic distance in **2a**. Similarly, at d = 2.472 Å, the CASPT2-optimized interallylic distance of **2c**, ΔE_{HL}(**2c**) = 23.3 kcal/mol and ΔE_{HL}(**2d**) = 35.8 kcal/mol. Thus, substitution of H in **2a** by F in **2b** and the CH_2 group in **2c** by O in **2d**, does, indeed, result in through-bond interactions that stabilize the HOMO, relative to the LUMO, and thus increase the size of ΔE_{HL}(**2a**) = 75.3 kcal/mol, the energy difference between these two orbitals.

(82) Review: Borden, W. T. *Chem. Commun.* **1998**, *18*, 1919.

(83) Due to the fact that the B3LYP wavefunctions for **2a** and **2b** are restricted, whereas the wavefunctions for **5a** and **5b** are not, the endothermicity of the reaction in eq 2 is underestimated by (U)B3LYP. In contrast, since the B3LYP wavefunctions for **2c** and **2d**, like those for **5c** and **5d**, are unrestricted, the UB3LYP BHASEs for **2c** and **2d** are much closer to the CASPT2 values.

(84) Roth, W. R.; Bauer, F.; Beitat, A.; Ebbrecht, T.; Wüstefeld, M. *Chem. Ber.* **1991**, *124*, 1453.

(85) Goldstein, M. J.; Benzon, M. S. *J. Am. Chem. Soc.*, **1972**, *94*, 7147.

(86) Hrovat, D. A.; Morokuma, K.; Borden, W. T. *J. Am. Chem. Soc.* **1994**, *116*, 1072.

(87) It is probably significant that, although the CASPT2 values of ΔE_{ST} and the BHASEs are nearly the same for **2a**, **c**, and **d**, ΔE_{ST} is larger than the BHASE by 2.1 kcal/mol in **2b**. In two molecules of **5b**, both nonbonding electrons are stabilized by their interaction with the C-F σ^* orbitals. However, in contrast, in the triplet state of **2b** the unpaired electron in the LUMO cannot interact at all with these σ^* orbitals. It seems likely that this is the reason why in **2b** ΔE_{ST} is larger than the BHASE value.

(88) It has previously been found[86] that use of a 6-311(2d,2p) basis set, which gives a bond dissociation energy of 66.0 kcal/mol, is necessary in order to obtain a bond dissociation enthalpy that agrees well with the experimental value of 59.6 ± 0.7 kcal/mol.[84]

(89) Dewar and Lo[65] were thus correct in conjecturing that strain relief is a major factor in the low barrier to degenerate rearrangement of **1a**.

(90) Reviews: (a) W. R. Dolbier, Jr. *Acc. Chem. Res.*, **1981**, *14*, 195; (b) B. E. Smart, In *Molecular Structure and Energetics*; eds. J. F. Liebman and A. Greenberg, VCH, Deerfield Beach, FL, **1986**; Vol 3, p 141.

(91) Unlike the case in **2c** and **2d**, the interallylic bond lengths at the optimized C_{2v} geometry of 2,8:4,6-bis(ethano)semibullvalene are actually slightly shorter than those in **2a**,[74] suggesting that the BHASE in the doubly-bridged C_{2v} semibullvalene is actually larger than that in **2a**. In fact, the (U)B3LYP singlet-triplet splitting of ΔE_{ST}=17.0 kcal mol that I compute for the bis(ethano)semibullvalene is larger by 4.7 kcal/mol than ΔE_{ST} in **2a.** Part of the larger value of ΔE_{ST} in the former semibullvalene is probably due to some residual repulsion between the two allyl radicals in the triplet. The ethano bridges constrain the interallyic distance in this state to be 2.301 Å, which is 0.284 Å shorter than the interallylic distance in the triplet state of **2a**. However, there is no doubt that bishomoaromatic stabilization, as well as strain relief, lead to 2,8:4,6-

bis(ethano)semibullvalene being predicted computationally to have a C_{2v} equilibrium geometry.[68,73,74]

Bibliography

Andersson, K.; Blomberg, M. R. A.; Fülscher, M. P.; Karlström, G.; Lindh, R.; Malmqvist, P.-Å.; Neogrády, P.; Olsen, J.; Roos, B. O.; Sadlej, A. J.; Schütz, M.; Seijo, L.; Serrano-Andrés, L.; Siegbahn, P. E. M.; Widmark, P.-O. *MOLCAS*, version 4.1; Department of Theoretical Chemistry, Chemical Centre: University of Lund, P.O.B. 124, S-221 00 Lund, Sweden, **1997**.

Andersson, K.; Blomberg, M. R. A.; Fülscher, M. P.; Karlström, G.; Lindh, R.; Malmqvist, P.-Å.; Neogrády, P.; Olsen, J.; Roos, B. O.; Sadlej, A. J.; Schütz, M.; Seijo, L.; Serrano-Andrés, L.; Siegbahn, P. E. M.; Widmark, P.-O. MOLCAS, version 5.0; Department of Theoretical Chemistry, Chemical Centre: University of Lund, P.O.B. 124, S-221 00 Lund, Sweden, **1997**.

Andersson, K.; Malmqvist, P.-Å.; Roos, B. O. *J. Chem. Phys.* **1992**, *96*, 1218.

Andersson, K.; Malmqvist, P.-Å.; Roos, B. O. *J. Chem. Phys.* **1992**, *96*, 1218.

Andersson, K.; Malmqvist, P-Å.; Roos, B. O.; Sadlej, A. J.; Wolinski, K. *J. Phys. Chem.* **1990**, *94*, 5483.

Andersson, K.; Malmqvist, P-Å.; Roos, B. O.; Sadlej, A. J.; Wolinski, K. *J. Phys. Chem.* **1990**, *94*, 5483.

Ashe, A. J., III, *Acc. Chem. Res.* **1978**, *11*, 153.

Ashe, A. J., III, Gordon, M. D. *J. Am. Chem. Soc.* **1972**, *94*, 7596.

B. E. Smart, In *Molecular Structure and Energetics*; eds. J. F. Liebman and A. Greenberg, VCH, Deerfield Beach, FL, **1986**; Vol 3, p 141.

Basemen, R. J.; Pratt, D. W.; Chow, M.; Dowd, P. *J. Am. Chem. Soc.* **1976**, *98*, 5726.

Becke, A. D. *J. Chem. Phys.* **1993**, *98*, 5648.

Benson, S. W. *Thermochemical Kinetics*, 2nd ed.; Wiley: New York, **1976**.

Bent, H. A. *Chem. Rev.* **1961**, *61*, 275.

Berger, S.; Brauman, J. I. *J. Am. Chem. Soc.* **1992**, *114*, 4737.

Berkowitz, J.; Ellison, G. B.; Gutman, D. *J. Phys. Chem.* **1994**, *98*, 2744.

Berson, J. A. In *Diradicals*; Borden, W. T., Ed.; J. Wiley and Sons: New York, **1982**; Chapter 4.

Berson, J. A. *Acc. Chem. Res.* **1978**, *11*, 446.

Bode, B. M.; Gordon, M. S. *J. Mol. Graphics Mod.* **1999**, *16*, 133.

Borden, W. T. In *Diradicals*; Borden, W. T., Ed.; J. Wiley and Sons: New York, **1982**; pp. 1-72.

Borden, W. T. *Chem. Commun.* **1998**, *18*, 1919.

Borden, W. T. In *Magnetic Properties of Organic Materials*; Lahti, P., Ed..; Marcel Dekker, Inc.: New York, **1999**; pp. 61-102.

Borden, W. T.; Davidson, E. R. *Acc. Chem. Res.* **1981**, *14*, 69.

Borden, W. T.; Davidson, E. R. *Acc. Chem. Res.* **1996**, *29*, 67.

Brook, A. G; Duff, J. H. *J. Am. Chem. Soc.* **1969**, *91*, 2119.

Chase, M. W., Jr. *NIST-JANAF Themochemical Tables, Fourth Edition, J. Chem. Phys. Ref. Data, Monograph 9*, **1998**.

Cheng, A. K.; Anet, F. A. L.; Mioduski, J.; Meinwald, J. *J. Am. Chem.Soc.* **1974**, *96*, 2887.

Cherry, W.; Epiotis, N. D.; Borden, W. T. *Acc. Chem. Res.* **1977**, *10*, 167.

Childs, R. F.; Cremer, D.; Elia, G. In *The Chemistry of the Cyclopropyl Group*; Rappoport, Z., Ed.; J. Wiley & Sons: Chichester, **1995**; Vol. 2, 411.

Clark, T.; Chandrasekhar, J.; Spitznagel, G. W.; Schleyer, P. v. R. *J. Comput. Chem.* **1983**, *4*, 294.

Coolidge, M. B.; Borden, W. T. *J. Am. Chem. Soc.* **1988**, *110*. 2298.

Coolidge, M. B.; Borden, W. T. *J. Am. Chem. Soc.* **1990**, *112*, 1704.

Coolidge, M. B.; Hrovat, D. A.; Borden, W. T. *J. Am. Chem. Soc.* **1992**, *114*, 2354.

Coulson, C. A. *J. Chim. Phys.* **1948**, *45*, 243.

Cowley, A. H. *Polyhedron* **1984**, *3*, 389.

Cowley, A. H. *Acc. Chem. Res.* **1984**, *17*, 386.

Cramer, C. J.; Smith, B. A. *J. Phys. Chem.* **1996**, *100*, 9664.

Curtiss, L. A.; Raghavachari, K.; Trucks, G. W.; Pople, J. A. *J. Chem. Phys.* **1991**, *94*, 7221.

Davidson, E. R.; Borden, W. T.; *J. Am. Chem. Soc.* **1977**, *99*, 2053.

Davidson, E. R.; Borden, W. T. *J. Phys. Chem.* **1983**; *87*, 4783.

Debye. Weast, R. C., Ed. *Handbook of Chemistry and Physics, 66th Edition*: CRC Press: Boca Raton, **1985**, E-59.

Dewar, M. J. S.; Jie, C. *Tetrahedron* **1988**, *44*, 1351.

Dewar, M. J. S.; Lo, D. H. *J. Am. Chem. Soc.* **1971**, *93*, 7201.

Ding, L.; Marshall, P. *J. Am. Chem. Soc.* **1992**, *114*. 5754.

Dolbier, W. R., Jr. *Acc. Chem. Res.*, **1981**, *14*, 195.

Dowd, P. *Acc. Chem. Res.* **1972**, *5*, 242.

Dowd, P. *J. Am. Chem. Soc.* **1966**, *88*, 2587.

Dowd, P.; Gold, A.; Sachdev, K. *J. Am. Chem. Soc.* **1968**, *90*, 2715.

Dowd, P.; Sachdev, K. *J. Am. Chem. Soc.* **1967**, *89*, 715.

Du, P.; Borden, W. T. *J. Am. Chem. Soc.* **1987**, *109*, 5330.

Feller, D.; Davidson, E. R.; Borden, W. T. *J. Am. Chem. Soc.* **1985**, *107*, 2596.

Frisch, M. J.; Trucks, G. W.; Schlegel, H. B.; Scuseria, G. E.; Robb, M. A.; Cheeseman, J. R.; Zakrzewski, V. G.; Montgomery, J. A., Jr.; Stratmann, R. E.; Burant, J. C.; Dapprich, S.; Millam, J. M.; Daniels, A. D.; Kudin, K. N.; Strain, M. C.; Farkas, O.;

Tomasi, J.; Barone, V.; Cossi, M.; Cammi, R.; Mennucci, B.; Pomelli, C.; Adamo, C.; Clifford, S.; Ochterski, J.; Petersson, G. A.; Ayala, P. Y.; Cui, Q.; Morokuma, K.; Malick, D. K.; Rabuck, A. D.; Raghavachari, K.; Foresman, J. B.; Cioslowski, J.; Ortiz, J. V.; Stefanov, J. V.; Liu, G.; Liashenko, A.; Piskorz, P.; Komaromi, I.; Gomperts, R.; Martin, R. L.; Fox, D. J.; Keith, T.; Al-Laham, M. A.; Peng, C. Y.; Nanayakkara, A.; Gonzalez, C.; Challacombe, M.; Gill, P. M. W.; Johnson, B.; Chen, W.; Wong, M. W.; Andres, J. L.; Gonzalez, C.; Head-Gordon, M.; Replogle, E. S.; Pople, J. A. *Gaussian 98, Revision A.6*; Gaussian, Inc.: Pittsburgh, PA, 1998.

Frisch, M. J.; Trucks, G. W.; Schlegel, H. B.; Scuseria, G. E.; Robb, M. A.; Cheeseman, J. R.; Zakrzewski, V. G.; Montgomery, J. A., Jr.; Stratmann, R. E.; Burant, J. C.; Dapprich, S.; Millam, J. M.; Daniels, A. D.; Kudin, K. N.; Strain, M. C.; Farkas, O.; Tomasi, J.; Barone, V.; Cossi, M.; Cammi, R.; Mennucci, B.; Pomelli, C.; Adamo, C.; Clifford, S.; Ochterski, J.; Petersson, G. A.; Ayala, P. Y.; Cui, Q.; Morokuma, K.; Malick, D. K.; Rabuck, A. D.; Raghavachari, K.; Foresman, J. B.; Cioslowski, J.; Ortiz, J. V.; Stefanov, J. V.; Liu, G.; Liashenko, A.; Piskorz, P.; Komaromi, I.; Gomperts, R.; Martin, R. L.; Fox, D. J.; Keith, T.; Al-Laham, M. A.; Peng, C. Y.; Nanayakkara, A.; Gonzalez, C.; Challacombe, M.; Gill, P. M. W.; Johnson, B.; Chen, W.; Wong, M. W.; Andres, J. L.; Gonzalez, C.; Head-Gordon, M.; Replogle, E. S.; Pople, J. A. *Gaussian 98, Revision A.7*; Gaussian, Inc.: Pittsburgh, PA, 1998.

Goldstein, M. J.; Benzon, M. S. *J. Am. Chem. Soc.*, **1972**, *94*, 7147.

Goren, A. C.; Hrovat, D. A.; Seefelder, M.; Quast, H.; Borden, W. T. *J. Am. Chem. Soc.* **2002**, *124*, 3469.

Goumri, A.; Yuan, W.-J.; Marshall, P. *J. Am. Chem. Soc.* **1993**, *115*, 2539.

Harihan, P. C.; Pople, J. A. *Theor. Chim. Acta* **1973**, *28*, 213.

Helgaker, T.; Jørgensen, P. Olsen, J. *Molecular Electronic-Structure Theory*: John Wiley and Sons, Ltd.: Chichester, **2000**.

Hoffmann, R.; Stohrer, W. D. *J. Am. Chem. Soc.* **1971**, *93*, 6941.

Hrovat, D. A.; Duncan, J. A.; Borden, W. T. *J. Am. Chem. Soc.* **1999**, *121*. 169.

Hrovat, D. A.; Morokuma, K.; Borden, W. T. *J. Am. Chem. Soc.* **1994**, *116*, 1072.

Hrovat, D. A.; Williams, R. V.; Goren, A. C.; Borden, W. T. *J. Comp. Chem.* **2001**, *22*, 1565.

Itoh, T.; Matsuda, K.; Iwamura, H.; Hori, K. *J. Am. Chem. Soc.* **2000**, *122*, 2567.

Jahn, H. A.; Teller, E. *Proc. R. Soc. London, Ser. A* **1937**, *116*, 605.

Jia, Z. S.; Brandt, P.; Thibblin, A. *J. Am. Chem. Soc.* **2001**, *123*, 10147.

Jiao, H.; Nagelkerke, R.; Kurtz, H. A.; Williams, R. V.; Borden, W. T.; Schleyer, P. v. R. *J. Am. Chem. Soc.* **1997**, *119*, 5921.

Johnson, W. T. G.; Borden, W. T. *J. Am. Chem. Soc.* **1997**, *119*, 5930.

Kemnitz, C. R.; Karney, W. L.; Borden, W. T. *J. Am. Chem. Soc.* **1998**, *120*, 3499.

Koch, W.; Holthausen, M. C. *A Chemist's Guide to Density Functional Theory, Second Edition*: Wiley-VCH: Weinheim, **2001**.

Komaguchi, K.; Shiotani, M.; Lund, A. *Chem. Phys. Lett.* **1997**, *265*, 217.

Kreil, C. L.; Chapman, O. L.; Burns, G. T.; Barton, T. J. *J. Am. Chem. Soc.* **1980**, *102*, 841.

Krusic, P. G.; Kochi, J. K. *J. Am. Chem. Soc.* **1969**, *91*, 3938.

Kutzelnigg, W. *Angew. Chem. Int. Ed. Engl.* **1984**, *23*, 272.

Lee, C.; Yang, W.; Parr, R. G. *Phys. Rev. B* **1988**, *37*, 785.

Maier, G.; Mihm, G.; Baumgartener, R. O. W.; Reisenauer, H. P. *Chem. Ber.* **1984**, *117*, 2337.

Maier, G.; Mihm, G.; Reisenauer, H. P. *Angew. Chem. Int. Ed Engl.* **1980**, *19*, 52.

Maier, G.; Mihm, G.; Reisenauer, H. P. *Chem. Ber.* **1982**, *115*, 801.

Märkl, G.; Lieb, F. *Angew. Chem. Int. Ed Engl.* **1968**, *7*, 733.

Märkl, G.; Schlosser, W. *Angew. Chem. Int. Ed Engl.* **1988**, *27*, 963.

Miller, L. S.; Grohmann, K.; Dannenberg, J. J. *J. Am. Chem. Soc.* **1983**, *105*, 6862.

Miyashi, T.; Kamata, M.; Mukai, T. *J. Am. Chem. Soc.* **1986**, *108*, 2755.

Miyashi, T.; Takahashi, Y.; Mukai, T.; Roth, H. D.; Schilling, M. L. M. *J. Am. Chem. Soc.* **1985**, *107*, 1079.

More O'Ferrall, R. A.; Rao, S. N. *Croat. Chem. Acta* **1992**, *65*, 593.

Moskau, D.; Aydin, R.; Leber, W.; Günther, H.; Quast, H.; Martin, H.-D.; Hassenrück, K.;

Miller, L. S.; Grohmann, K. *Chem. Ber.* **1989**, *122*, 925.

Nicolaides, A.; Borden, W. T. *J. Am. Chem. Soc.* **1991**, *113*. 6750.

Ovchinnikov, A. A. *Theoret. Chim. Acta* **1978**, *47*, 297.

Quast, H.; Janiak, R.; Peters, E.-M.; Peters, K.; von Schnering, H. G. *Chem. Ber.* **1992**, *125*, 969.

Quast, H.; Seefelder, M. *Angew. Chem. Int. Ed.* **1999**, *38*, 1064.

Raabe, G.; Michl, J. *Chem. Rev.* **1985**, *85*, 419.

Rao, S. N.; More O'Ferrall, R. A.; Kelly, S. C.; Boyd, D. R.; Agarwal, R. *J. Am. Chem. Soc.* **1993**, *115*, 5458.

Römer, B.; Gatev, G. G.; Zhong, M.; Brauman, J. I. *J. Am. Chem. Soc.* **1998**, *120*, 2919.

Roth, W. R.; Bauer, F.; Beitat, A.; Ebbrecht, T.; Wüstefeld, M. *Chem. Ber.* **1991**, *124*, 1453.

Sakurai, H.; Murakami, M. *J. Am. Chem. Soc.* **1969**, *91*, 519.

Schmidt, M. W.; Baldridge, K. K.; Boatz, J. A.; Elbert, S. T.; Gordon, M. S.; Jensen, J. H.; Koseki, S.; Matsunga, N.; Nguyen, K. A.; Su, S. J.; Windus, T. L.; Dupuis, M.; Montgomery, J. A. *J. Comput. Chem.* **1993**, *14*, 1347.

Schmidt, M. W.; Truong, P. N.; Gordon, M. S. **1987**, *109*, 5217

Schmidt, M. W.; Truong, P. N.; Gordon, M. S. **1987**, *109*, 5217.

Sun, H.; Hrovat, D. A.; Borden, W. T. *J. Am. Chem. Soc.* **1987**, *109*, 5275.

Takahashi, Y.; Miyashi, T.; Mukai, T. *J. Am. Chem. Soc.* **1983**, *105*, 6511.

Tantillo, D. J.; Hoffmann, R. *J. Org. Chem.* **2002**, *67*, 1419.

Tokitoh, N.; Wakita, K.; Okazaki, R.; Nagase, S.; Schleyer, P. von R.; Jiao, H. *J. Am. Chem. Soc.* **1997**, *119*, 6851.

Walsh, R. A. *Acc. Chem. Res.* **1981**, *14*, 246.

Wenthold, P. G.; Hu, J.; Squires, R. R.; Lineberger, W. C. *J. Am. Chem. Soc.* **1996**, *118*, 475.

Wenthold, P. G.; Hu., J; Squires, R. R; Lineberger, W. C. *J. Am. Soc. Mass Spectrom.* **1999**, *10*, 800-809.

Wetzel, D. M.; Salomon, K. E.; Brauman, J. I. *J. Am. Chem. Soc.* **1989**, *111*, 3835.

Wiberg, K. B.; Nakaji, D. *J. Am. Chem. Soc.* **1993**, *115*, 10658.

Wiberg, K. B.; Nakaji, D. *J. Am. Chem. Soc.* **1993**, *115*, 10658.

Williams, R. V. *Adv. Theor. Interesting Mol.* **1998**, *4*, 157.

Williams, R. V. *Chem. Rev.* **2001**, *101*, 1185.

Williams, R. V. *Eur. J. Org. Chem.* **2001**, 227.

Williams, R. V.; Gadgil, V. R.; Chauhan, K.; Jackman, L. M.; Fernandes, E. *J. Org. Chem.* **1998**, *63*, 3302.

Williams, R. V.; Kurtz, H. A. *J. Chem. Soc. Perkin Trans. 2* **1994**, 147.

Williams, R. V.; Kurtz, H. A. *J. Org. Chem.* **1988**, *52*, 3226.

Wu, Y.-D.; C.-H. Ling, *J. Org. Chem.* **1995**, *60*, 821.

Vita

Eric Brown was born in Normal, Illinois. He earned a Bachelor of Science degree from Illinois State University, a Master of Science degree from the University of Washington, and a Doctor of Philosophy from the University of Washington.